UNIVERSITY OF WEST BOHEMIA IN PILSEN
FACULTY OF APPLIED SCIENCES
DEPARTMENT OF MECHANICS

DIPLOMA THESIS

Versatile sport helmet

Plzeň, 30.5.2014 Bc. Richard Hynek

0.1 Declaration

I hereby certify that this diploma thesis is entirely the result of my work and I faithfully and properly cited all sources used in the thesis.

In Pilsen, 30.5.2014

0.2 Acknowledgements

I would like to cordially thank all the people who enabled the creation of this thesis. That includes my supervisor Ing. Radek Kottner, Ph.D. to who I thank for his carefull corrections and fitting comments. It also involves all other stuff of the Department of Mechanics who creates friendly workplace for all the students. Namely I would like to thank Ing. Tomáš Mandys, Ing Jan Bartošek and Ing. Jan Krystek, Ph.D. who significantly participated in experiments needed in this thesis. But principally, I deeply thank my parents and my family who supported me in all the ways during my studies.

0.3 Abstract

Richard Hynek, Department of mechanics, Faculty of applied sciences, University of West Bohemia in Pilsen

Abstract of diploma thesis

Versatile sport helmet

The aim of this work is to design a versatile helmet for various sports using modern materials and design procedures. In the first three chapters, the work is focused on analysis of the current market state, helmet cosntructions, safety requirements, potentiall users and their demands. The fourth chapter concerning materials is focused on the carbon fibre reinforced plastics, expanded polystyrene and D3O. It deals with analytical and numerical finite-element modeling of these materials and compression and impact experiments. The results of these experiments were needed for the identification of parameters of material models by optimization algorithm. The final chapter is focused on the design of the versatile helmet reflecting the selected materials and the requirements obtained in the analysis in the first chapters. The last part of the chapter deals with finite element modeling of the standartized impact tests of the final helmet design and evaluation of the results.

Keywords: versatile helmet, user value analysis, CFRP, EPS, D3O, Finite Element Analysis, elastoplastic model, viscoelastic model, Hashin criterion, EN 1078, EN 12 492, EN 1384, EN 966, EN 1077, EN 1385.

0.4 Abstrakt

Richard Hynek, Katedra mechaniky, Fakulta aplikovaných věd, Západočeská univerzita v Plzni

Abstrakt diplomové práce

Multifunkční sportovní přilba

Cílem této práce je navrhnout univerzální přilbu pro více různých sportů s použitím moderních materiálů a návrhových postupů. V prvních třech kapitolách byla provedena analýza současného stavu trhu se sportovními přilbami, konstrukcí přileb, bezpečnostních nároků, potenciálních uživatelů a jejich požadavků. Čtvrtá kapitola práce, týkající se materiálů použitých k návrhu přilby, je zaměřena na vláknové uhlíkové kompozity, expandovaný polystyren a D3O. Zabývá se analytickými a numerickými konečněprvkovými modely těchto materiálů a tlakovými a rázovými experimenty. Výsledky experimentů byly použity pro identifikaci parametrů materiálových modelů pomocí optimalizačního algoritmu. Závěrečná pátá kapitola je zaměřena na návrh multifunkční přilby reflektující vybrané materiály a požadavky vzešlé z analýzy uživatelů. Její závěrečná část se týká modelování normalizovaných zkušebních testů metodou konečných prvků a vyhodnocení výsledků.

Klíčová slova: multifunkční přilba, analýza uživatelů, CFRP, EPS, D3O, Metoda Konečných Prvků, elastoplastický model, viskoelastický model, kritérium Hashin, EN 1078, EN 12 492, EN 1384, EN 966, EN 1077, EN 1385.

Contents

List of Figures

List of Tables

List of abbreviations and symbols

a - Acceleration $[m/s^2]$
e - Deformation in Zener model [-]
$\overline{e}$ - Constant value of deformation in Zener model [-]
e_s - Deformation of serial spring in Zener model [-]
e_d - Deformation of serial damper in Zener model [-]
E_{11} - Youngs's modulus of fibre composite in the longitudinal direction [Pa]
E_{22} - Youngs's modulus of fibre composite in the transversal direction [Pa]
E_{33} - Youngs's modulus of fibre composite in the second transversal [Pa] direction
E - Youngs's modulus [Pa]
E^{d3o} - Youngs's modulus of D3O [Pa]
E^{eps} - Youngs's modulus of EPS [Pa]
E_S - Youngs's modulus of serial spring in Zener model [Pa]
E_∞ - Youngs's modulus of EPS of paralell spring in Zener model [Pa]
F_f^t - Failure index of composite for the tensile fibre failure mode [-]
F_f^c - Failure index of composite for the compressive fibre failure mode [-]
F_t^m - Failure index of composite for the tensile matrix failure mode [-]
F_c^m - Failure index of composite for the compresiive matrix failure mode [-]
F_i^{exp} - Force in the time i in experiment [N]
F_i^{mod} - Force in the time i in model [N]
$\overline{g}_i^P$ - Shear relaxation modulus ratio in threedimensional viscoelastic model [-]
G_{12} - Shear modulus of fibre composite in the plane of lamina [Pa]
G_{13} - Shear modulus of fibre composite in the plane defined by longitudinal and perpendicular directions [Pa]
G_{23} - Shear modulus of fibre composite in the plane defined by transversal and perpendicular directions [Pa]
G_{ft}^C - Energy dissipated in the tensile damage of the fibre $[J/m^2]$
G_{fc}^C - Energy dissipated in the compressive damage of the fibre $[J/m^2]$
G_{mt}^C - Energy dissipated in the tensile damage of the matrix $[J/m^2]$
G_{mc}^C - Energy dissipated in the compressive damage of the matrix $[J/m^2]$
$G_R(t)$ - Relaxation modulus in threedimensional viscoelastic model [-]
k - Yield stress ratio for compressive loading [-]
k_t - Yield stress ratio for hydrostatic loading [-]
$\overline{k}_i^P$ - Bulk relaxation modulus ratio in threedimensional viscoelastic model [-]
S_i - Stress value belonging to certain value of plastic strain in plastic curve [Pa]
S_T - Transversal shear strength of the fibre composite [Pa]
t - Time [s]
T_e - Relaxation time [-]
v - Velocity $[m/s]$
V_f - Volume ratio of the fibre in composite [-]
V_m - Volume ratio of the matrix in composite [-]
X_T - Longitudinal tensile strength of the fibre composite [Pa]
X_C - Longitudinal compressive strength of the fibre composite [Pa]
Y_T - Transversal tensile strength of the fibre composite [Pa]
Y_C - Transversal compressive strength of the fibre composite [Pa]

γ - Relaxation coefficient in Zener model [-]

η - Viscosity of serial damper in Zener model [Pa]

ν_{12} - Poisson's ratio of fibre composite in the plane of lamina [-]

ν_{13} - Poisson ratio of fibre composite in the plane defined by longitudinal and perpendicular directions [-]

ν_{23} - Poisson's ration of fibre composite in the plane defined by transversal and perpendicular directions [-]

ν^{d3o} - Poisson's ratio of D3O [-]

ν^{eps} - Poisson's ratio of EPS [-]

ν_f - Poisson's ratio of the fibre [-]

ν_m - Poisson's ratio of the matrix [-]

ρ - Density $[kg/m^3]$

$\overline{\sigma}_{11}$ - Stress in the fibre composite in the longitudinal direction [Pa]

$\overline{\sigma}_{22}$ - Stress in the fibre composite in the transversal direction [Pa]

$\overline{\sigma}$ - Stress in Zener model for constant value of deformation [Pa]

σ_S - Stress in the serial branch in Zener model [Pa]

τ - Stress in Zener model [Pa]

$\overline{\tau}_{12}$ - Shear stress in the fibre composite in the plane of lamina [Pa]

Chapter 1

Introduction

1.1 Background

Human inventiveness is limitless even at the fied of the sport activites. Every single year many new sports are invented and even more are shifted to the level that seemed to be impossibe a few years ago. New sport branches are faster, more dynamic, more agressive and so more dangerous. Although human body is a remarkable miracle, it could not stand such a sport progress without the help of the modern technology. It could be various devices and equipment (bikes, skates, rackets, ski, trainers, paraglides...), clothes, revitalization care, food but also the insurance for the case that not everything goes as planned – protective equipment.

One of the oldest tools preventing the serious injuries is a helmet. Originally invented for the needs of warriors thousands of years before the first sport. The original helmets prevented their users from the penetration by sharp objects only. Today's models are far more sophisticated whether we are talking about soldier‘s, construction worker‘s or sportsmen‘s helmets. Thanks to the huge differencies among the human activities, where the helmet is needed, also it's general and technical specifics are sometimes very divergent. To understand the basic needs of today's users, the analysis of activies was performed. The aim was to find out whether there are activities that share so similar head protection specifics that one type of helmet could be used for all of them.

1.2 Thesis objective

Another present trend is the wide focus of the amateur sportsmen. It is probably determined by wider offer of the sports, gradually improving economical situation and more available sport equipment. Nevertheless, we also live in the era when the certain part of population starts to think efficiently and thrifty even in the daily problems. And need to have a special helmet model for all the sport activities is financially, spatially and time inefficient for the amateur sportsman. Therefore, the aim of this work was to find out if there could be one multifunctional helmet for such a person and to propose a generall design.

Remarkable technologies of today can produce almost anything from any material. Theoretically speaking, designer has a choose from the neverending scale of the materials whose usage could be a breakthrough on the first sight. On the other hand, an industry

producing the protective equipment is inovating slowly, which is caused by robustness of the manufacturing, rentability of the products and the current state of the market. Thus, it was crucial to find a healthy compromise between the strong inovation and the potential competitiveness.

The following work consists of several chapters that chronologically describe the whole design process - starting by state of the field of the helmets, through the analysis of the users and requirements, proposal of the materials for the key helmet segments (including investigation and modeling of the particular materials, validation of combined material model and the final design chapter that consists of the sketches, computer aided design (CAD) virtual model and the finite element (FE) calculation of the standartized helmet impact tests.

1.3 Technical challenges

The chapter regarding the key helmet segments is focused on the analysis of the materials that could be advantageously used in the design of the versatile helmet and modeling of these materials by Finite Elemet Method (FEM). In particullar, composite materials and materials with significant ability to absorb the mechanical energy. The usage of virtual FE material models can make design process more efficient and cheaper. Modeling was focused mainly on the impacts.

Final design chapter is focused on the design of the helmet from the the first sketches, respecting analysis from the first chapters, up to the complex threedimensional CAD model.

When a helmet is introduced to the market it is critical whether it meets standards of the particular market - european one in this case. These standards can be relatively comprehensive. Unfortunatelly, it is not in the range of this work to cover the entire design process. Consequently, some details were not considered which is mentioned at the appropriate places in the text. The parts of the standards regarding the impact test were taken as the main safety criterion. These standartized tests were modelled using FEM and evaluated.

1.4 Personal motivation

My great motivation in this work was the fact that I am personally widely focused amateur sport lover and there was no product on the current market matching all my requirements. Simultaneously, I wanted to use this topic for the practicall application of my theoretical background that I gained during my master studies of Industrial design at the Department of mechanics and during sessions of Product design in the scope of my studies at Faculty of Engineering of Manchester Metropolitan University. I let the reader to find whether this goal was achieved.

Chapter 2

State of art

2.1 History

The oldiest helmets were used by soldiers and found in the area of Asyria 900 B.C. Soldiers had worn thick leather or bronze helmets to prevent their heads in the fight from the blunt objects, sword's blades or arrow's tips. This basic approach has not changed for a thousand years. We can observe attempts of the basic ergonomy on well-preserved greek (400-300 B.C.) and roman (100 A.C.) soldier helmets where side and neck parts of the helmet were attached by the basic hinges that enabled easier head movements. Military helmets were frequently used as the distictive elements on (or out of) the battlefield, therefore, they were lavishly decorated. Helmets started to be used as a protection in sports and workplaces during the 19th century.

In general, every sport branch where the head protection is needed has it's own history of the helmets that in detail could exceed the scope of this work. Cycling was chosen as an example because it is one of the oldest sport branches and the best lightweight technologies were always used in the cycling helmets production.

On the edge of 19th and 20th century, when cyclist rode primarily velocipeds and the traffic was as dense as the network of the asphalt roads, cyclists used "helmets" made of strips of soft leather stuffed with a wool (Fig. 2.1).

Figure 2.1: Leather strip helmet from the begining of the cycling era in the end of 19th century. [1]

Also helmets with a stiff outer shell, mostly without any ventilation, was being used in the next decades . The next giant breakthrough was made in the 80's when helmets made of formed EPS (Expanded Polystyrene). The interesting fact is that these first EPS helmets were derived from the model that has been developed by american company Bell that has been used for the protection of the children after head's surgery for the common activities like walking (Fig. 2.2). Even thought this was significant step forward in head's protection, it has been very soon found out that helmets made of EPS itself are being damaged by brittle crack before depletion of it's protective potential - plastic deformation. The mainstream of the 90's and the beginning of the 20th century was focused on evolution of the EPS helmets. Results of this evolution are summarized in the following paragraphs.

Figure 2.2: Helmet made of expanded polystyren (EPS), the beginning of 80's. [1].

2.2 Current technical solutions

Even thought today's sport helmet market is very divers at the first sight and many specialized helmet types are available, they can be devided into three basic groups according to the technical solution used in the helmet design.

2.2.1 Hardshell

In this case helmet contains of the stiff outer shell that can be made of hardened plastic, light metal or composite material and it's thickness can be in milimeters. As written earlier, this layer is supposed to distribute the impact loading (that can be point-concentrateded in the worst case) to the wider surrounding, absorb the shock energy and prevent the fatal skull injuries. This layer is usually supported by the inner textile lining (foam insoles) (Fig. 2.3) that ensures user's comfort and in a small scope also helps with absorption of the impact energy (for example hockey or watersport helmets). The next option is the plastic clamping system that keeps a space of centimetres between thee outer shell and the user's head (some kinds of climbing and working helmets) (Fig. 2.4). This approach is being used mainly for it's low weight and for applications where the thick layer of the absorption liner is not wanted or it is unnecessary.

Figure 2.3: Typical hardshell helmet - a composite solution with the textile liner produced by Paraevoluce [2].

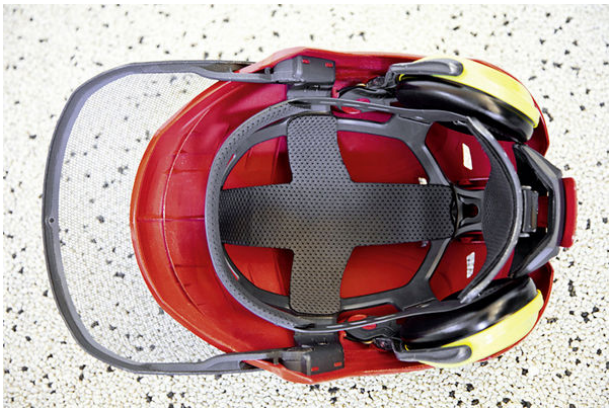

Figure 2.4: Work model with the plastic clamping system produced by Protos [3].

2.2.2 Hardshell + liner

It is the design solution that shares the key construction element with pure Hardshell version - the stiff outer shell. The shell is present for the same reasons as mentioned above but does not distribute the impact loading directly to the textile lining and then the user's skull but through the layer of the mechanical energy absorption material - so called liner. Expanded polystyrene (EPS) injected to the mould is the most widespread type of the liner these days. The layer of the liner is then connected with the outer shell mostly by adhesive joints. During the impact, the most of the energy is distributed by the outer shell into the liner and then disipated by the plastic deformation. Some part of the energy can also be absorbed by the shell damage especially when it is made of a fiber composite (see Fig. 2.6).

The advantage of this design solution is a high durability especially when the helmet is being treated rouhgly (the shell neither the liner are usually damaged during the low energy impacts), good ability to spread the loading into the wide area of liner and also the relatively low price. These helmets are also rarely broke by brittle damage even during the high energy impacts. This technology is normally used for the helmet categories, where the high energy impacts are supposed to happen (downhill skiing, downhill mountain biking,

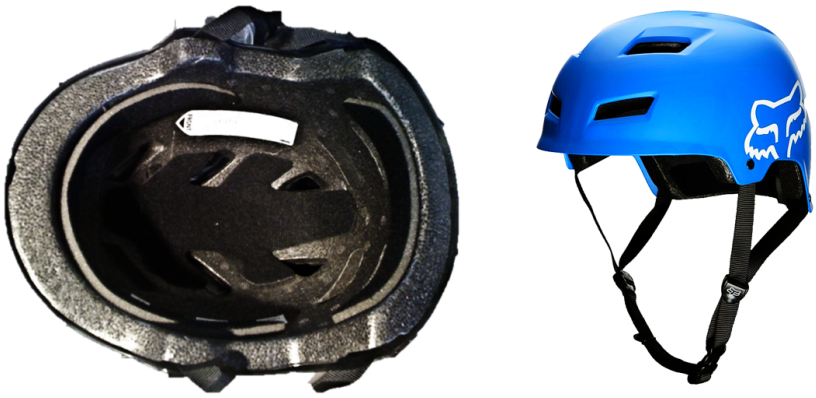

Figure 2.5: Typical hardshell helmet with EPS liner - model Transition Hard Shell produced by Fox [4]

dirtjump, skateboarding...) (Fig. 2.3)

Figure 2.6: Carbon composite hardshell equestrian helmet - "Carbon Air Cap" by Dainese [5].

2.2.3 In-molded EPS

In- molding is a customary name of technology that uses a very thin plastic outer shell (measured in fractions of milimeter) that is filled by melted polystyren under the pressure. Direct and durable connection between the plastic shell and the EPS liner is then attained (Fig. 2.7). In the past days, adhesives were used for the connection of the outer shell and the liner but these days the vast majority of the quality helmets is produced by the injection moulding into the shell. The thin outer layer has the similar objective as in the solutions mentioned above - the distribution of the loading into the wider area. Simulateously, it helps to incease the stiffness of the whole helmet, but in many cases does not cover all the EPS outer surface.

One of the current trends is the usage of the plastic or fiber composite skeleton that is melted into the EPS liner and that significantly increases the stiffness and the impact loading distribution ability (Fig. 2.8). Nevertheless, so far just in the top models. Almost always is the sequence concluded by the comfort textile lining.

The impact energy is there also absorbed by the plastic deformation but frequently also by the fraction damage of the liner especially during the high energy impacts. In graph on Fig. 2.9, significant difference can be observed in the acceleration measured in the headform (when the same impact test modelled) between pure EPS, in-molded EPS and in molded EPS with the theoretical inner shell 2.9.

Figure 2.7: Analysis of in-molded cycling helmet produced by Limar. An adhesive connection of polystyrene cells and plastic liner can be seen on the right figure.

Figure 2.8: In-molded Giro helmet with inner plastic skeleton.

Thus, it can be claimed that even a very thin plastic outer shell has a crucial influenece on the protective properties of the helmet. The advantage of the in-molded helmets is very low weight and possibility of various shaping (attractive design, functional elements, ventilation). The possible disadvantage is that in-molded helmets are more sensitive to the rough treatment and their structure can be damaged even by the low energy impact for example by sharp object - the outer shell is penetrated and the notch inside the liner can

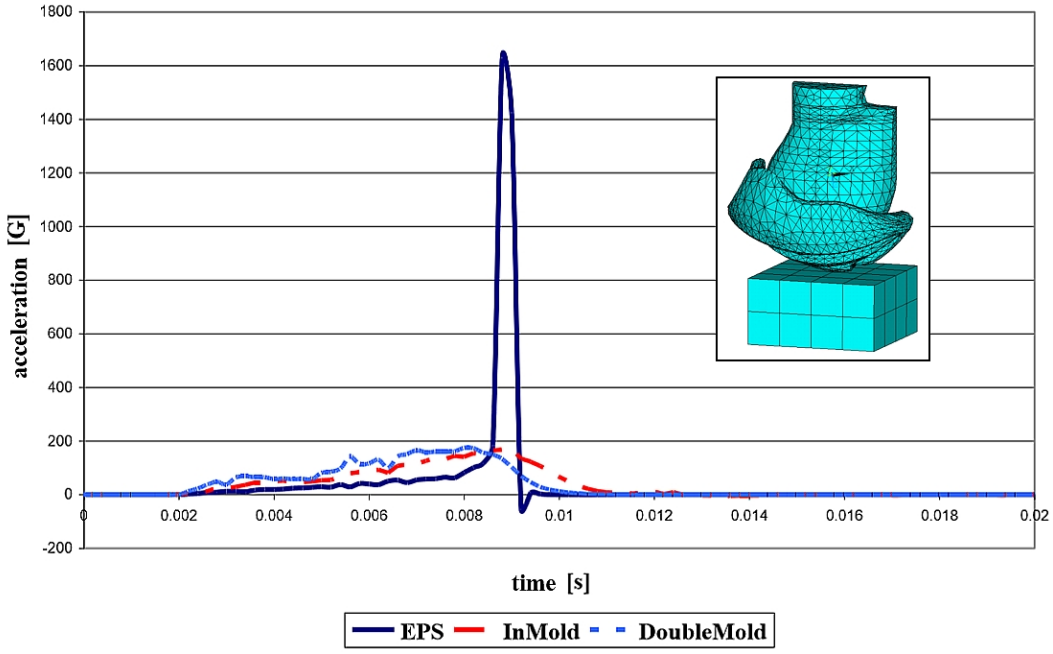

Figure 2.9: The difference in acceleration in the headform from FE analysis of the impact test in ANSYS. [6]

initiate the fracture earlier before the depletion of the plastic deformation. Despite that, the technology of in-molding in mass production has a really good ratio of price, weight and level of protection, therefore, it is being used in the wide spectrum of the helmets (almost all categories of cycling, some skiing and climbing models). In comparison with hardshell, in-molded helmet is usually the more expensive one.

2.3 New trends

Beside the main design solutions mentioned above there are attempts of established and completely new companies to enter the market with a highly innovative solutions. Generally, these innovations mostly concerns the helmet energy absorption liners. So called honeycomb constructions, that are very promising in the motorcycling helmets, are made of thin hexegonal or circular profiles (tubes) that have their axle oriented perpendicularly to the surface of the helmet. The energy disipation is ensured by it's damage evolution, mostly the plastic deformation. The main advantage comparing to the EPS liners is a lower or equal weight and better air ventilation. It is frequently used in the combination with EPS (Fig. 2.10).

Bike equipment brand Kali develops double liner solution where two layers of the different density are connected by the conical protrusions. Kali thinks it will lead to a higher safety for the high-energy impacts (Fig. 2.11).

Figure 2.10: The combination of the honeycomb structure and EPS in Smith Forefront helmet [7]

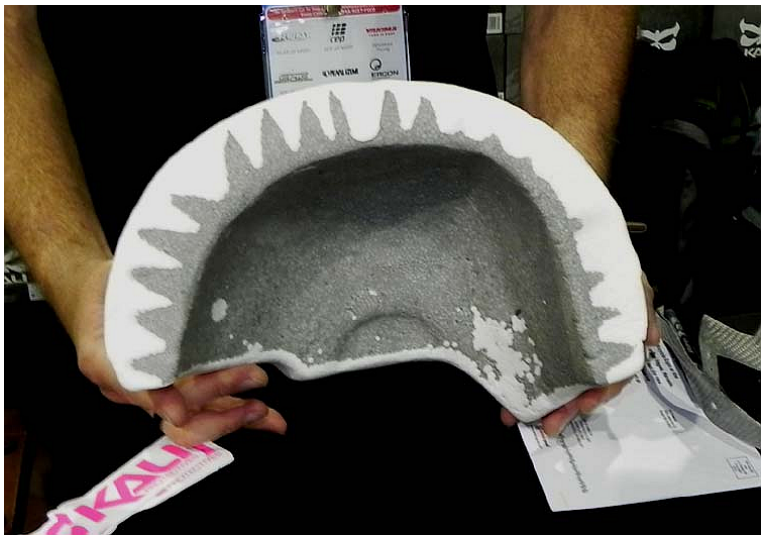

Figure 2.11: Double density liner produced by Kali [1].

Completely different approach was introduced in the project of two swedisch designers Anna Haupt and Therese Austin called Hövding. It is more like an airbag for cyclists hidden inside a collar than the helmet (Fig. 2.12). Hövding contains battery pack, accelerometer, evaluation software unit and the airbag itself. If the cycling airbag is going to take it's place on the market or if it is going to be a blind evolution branch will be clear soon. Hövding was brought to the market in 2013.

Some brands like POC are investing in the solution that should keep user's brain protected before the dangerous injuries caused by the rotational movement after non-perpendicular impact (Fig. 2.13). Some of their helmets contains two "outer" shells that can "slide" on each other and thus prevent the brain from the rotation.

Figure 2.12: Cycling airbag Hövding [9].

Figure 2.13: 'Multi impact protection system' (MIPS) in the helmet by POC [8].

2.4 The state of the market

It is not simple to analyze today's sport helmet market. There is no worldwide or national association that is focused directly on the sport helmets. It is possible to deduce some trends from the statistical data of a particular sport branches. But even there the helmets are mostly included in the general group of accesories with the other equipment or clothing.

American Bicycle Helmet Safety Institute (BHSI) did an interesting comparations of the safety of the helmets of the different price levels. They compared the cheap budget supermarket helmets in the span of 10 to 20 dolars and the branded helmets in the span of 150 to 210 dolars of the different pruducers. The construction of the tested helmets was EPS (bonded or in-molded). Institute let the tests performed by the certified lab CPSC (Consumer Product Safety Comission). Every helmet was droped with the standartized head mock up to the flat surface (1,2 metres) or the flat and spherical surface (0,5 metres). The results of the tests can be seen in Tab 2.1. Focusing just on the safety that can be

measured by the certified tests, all the helmets from all the price categories were equal. Good news are that even the cheapest helmets fulfilled the safety standards. The less expected fact is that even the expensive helmets have no added value in the mesureable safety.

Test type	Budget helmets	Expensive helmets
All tests averaged	101	104
Low velocity tests averaged	65	69
Low velocity - flat impactor	86	87
Low velocity - spherical impactor	47	47
High velocity tests averaged	137	146
High velocity - flat impactor	186	180
High velocity - spherical impactor	91	113

Table 2.1: Values of deceleration [G] in BHSI tests for the different price levels of the helmets. [1]

2.5 Motivation for a new solution

It could look like today's sport helmet market is highly diversificated and every potential user could find a model that fits his demands. Ironically, that is one of the disadvantages especially for the specific wide group of users. This group consists of a people who are an active sportsmen in many fields but far from the proffesional level. These people need many kinds of protection helmets. More exactly - they don't need them, but today's market does not offer one solution, one design that fits to the wide spectrum of sport activities. A model example could be an active sportsman, who participates hobby enduro bicycle events, his training includes the road cycling, who few times a year rides a wildwater, who also likes climbing and who likes downhill skiing in the winter time. If this model example would make a compromise in the comfort and use the climbing helmet for wildwater and climbing (that is frequent thing) he or she would has to own 4 different helmets. There is also a frequent situation when the sports are combined (riding the bike into the location of the next activity...). Thus, using many types of the helmets is disadvantageous and expensive for the most of potential target users that this work is focused on.

Chapter 3

Analysis of requirements and users

3.1 Analysis of potential users

Every single user or customer professes a different values and has a different needs that should be reflected in the design as much as possible, if the product is wanted to succeed. Prototype of the user that the final helmet from this work should fit to, could be defined as an universal and active amateur athlete.

3.1.1 Value analysis

Even after this group of users is defined, it still consists of very different customers. The estimation premises that the most of this users are in the middle or slightly above the average of incomes and have a time flexible job that enables to devote to their sport hobbies. They live by the modern 21st century life which pays (besides consumption) attention to the speed, dynamics and effectivity (low wastage, thrift). When this potential user decides about a purchase of any product he/she will not be probably looking for an exclusivity or the cheapest options on the other hand. He will require the smart, efective solution that saves his time and money.

Thus, one can summarize the main general goals of the universal sport helmet for an active universal athlete:

- High level of quality and manufacture
- Verified safety and comfort
- Realistic reasonable price
- Not extravagant, but interesting appearance
- Easy and quick setup and manupulation
- Versatility, not overcombination
- Reasonable number of features

3.2 Selection of combinable activities

To be able to decide about the versatility of the design it was neccessary to devide human activities in which some kind of the head protection by the helmet is needed and then consider very specific needs and protection requirements of these activities. Fig. 3.1 shows the first basic partition of the activities whereas the activities assumed to have similar requirements are marked green. In the scope of this basic analysis it was decided to develop more detailed list of the sport and other activities.

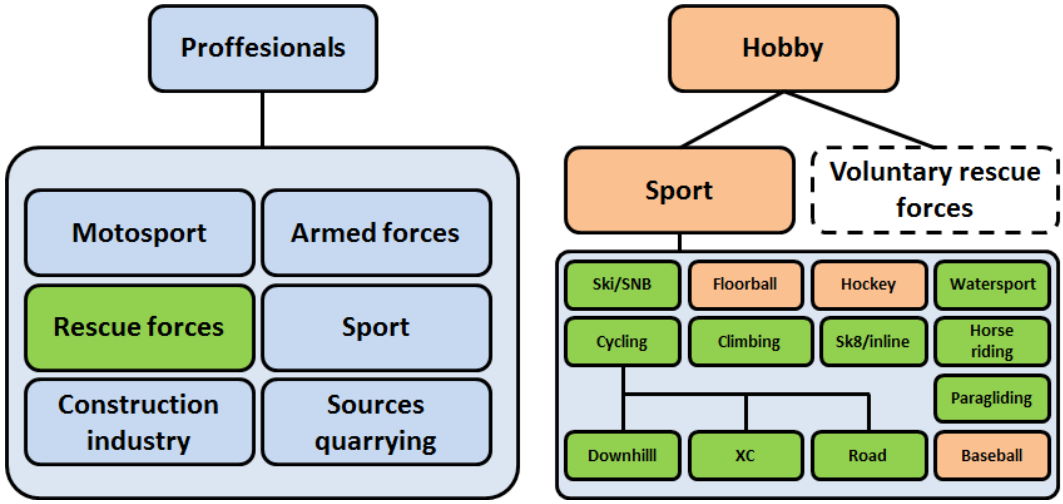

Figure 3.1: Basic partition of activities in which the head protection is needed.

These more detailed activities were entered into the table. Rows contains the properties (primary and secondary), columns contains the particular activities. An empty table was given to ten people including author of this work in order to fill it independently. The result is the table on Fig. 3.2. There is no mathematical tool to decide about the most importatnt properties and the possibility of usage of the one helmet for more activities. Even the first estimations are subjective because the wanted properties were chosen by the people in the roles of the potential customers. One of the auxiliary tools is the sum of occurences of the wanted properties for the particular activity and vice versa. It helps to identify which properties occurs the most frequently in the whole list of activities.

Using the results of this analysis, the list of activites (author believes the versatile helmet can be designed for) was created:

- Cycling
- Inline skating and skateboarding
- Mountaineering
- Horse riding
- Skiing a snowboarding
- Paragliding
- White water sports

Figure 3.2: Helmet property analysis.

3.3 Selection of required properties.

Based on the analysis of the table of the activities and properties, it is possible to designate basic required market, functional and visual features of the helmet:

Primary features:

- Low weigth
- Ventilation
- High protection factor
- Adaptibility on more head sizes in the certain scale.
- Ability to connect accesories (headlights, cameras, external bateries, glasses...)
- Durability
- Low volume
- Easy and quick adjustment

Secondary features:

- Removeable inner cushion
- Easy control and adjustment (even if wearing gloves)
- Protective net in the ventilation holes
- Bright colors
- Ear protection
- Chin protector
- Peak
- Reflective elements
- Possibility of using fullface googles.
- Sealing of the ventilation holes

It is neccessary to mention that even after the carried analysis some of the features can still be in conflict. Therefore one have to decide about the reasonable compromise during the design process.

3.3.1 European standards ČSN EN

The Czech or european legislation devides the protective helmets into the several categories whereas for each one of them testing processes and limit values of the results are specified. Every helmet signed CE (certified for european market) has to pass this standard. Considering the groups defined as the target in the previous text, the final helmet design should pass these standards:

- ČSN EN 1078 - Helmets for pedal cyclists and for users of skateboards and roller skates
- ČSN EN 12 492 - Helmets for mountaineers
- ČSN EN 1384 - Helmets for equestrian activities
- ČSN EN 966 - Helmets for airborne sports
- ČSN EN 1077 - Helmets for alpine skiers and snowboarders
- ČSN EN 1385 - Helmets for canoying and white water sports

Each standard specifies several key values that has to be observed during the testing. Almost all mentioned standards determine the maximal value of decceleration in G $[9.82m.s^{-2}]$ as the main safety condition. The values are measured in the center of mass of the human head mockup whose shape and properties are defined by ČSN EN 960 standard. Tab. 3.1 sums up mentioned standards including the processes of the testing and the limit values.

Standard	Main measured value	Limit value	Measurement method	Other aspects
ČSN EN 1078	Maximal deceleration	250 G	Flat anvil impact (velocity v = 5.42 m/s), corner anvil impact (v = 4.57 m/s)	Helmet slipping, strength of the chin straps
ČSN EN 12 492	Maximal transmitted force	10 kN	Free fall impact vertical (fall heigth h = 2m), frontal, lateral and rear (h = 0.5m))	Helmet slipping, strength of the chin straps, penetration
ČSN EN 1384	Maximal deceleration	250 G	Free fall impact, flat anvil (h = 1.5m)	Helmet slipping, strength of the chin straps, penetration
ČSN EN 966	Maximal deceleration	250 G	Free fall impact, flat anvil (h = 1.5m)	Helmet slipping, strength of the chin straps, penetration, head mobility, visibility
ČSN EN 1077	Maximal deceleration	250 G	Flat anvil impact (v = 5.42 m/s)	Helmet slipping, strength of the chin straps, penetration
ČSN EN 1385	Maximal deceleration	250 G	Hemisphere anvil impact (v = 3.11 m/s)	Helmet slipping, strength of the chin straps, penetration, floating

Table 3.1: The sum of the helmet standards related to this work [11]

Chapter 4

Helmet key segments

4.1 Outer shell - composite

Composite material is defined as material that macroscopically consists of two or more components of different properties. In the most cases some components are dominant in the strength or other required property (for example fibers). Those are surrounded by matrix. Generally, composites can be anisotropical but in the most cases the situation is simplified by the planes of symmetry.

As mentioned in the Current solutions, the right choice of the outer shell is crucial for the helmet's proper function. Shells made of fibre composite are usually used in the design of motorcycle, downhill or light paraglide helmets. Technically, they belong among the hardshell helmets. Besides good ability to spread the impact loading, the fibre composite shells (especially those made of carbon fibres) are penetration resistant, thanks to the fibres they can hold the rest of the helmet together even when heavily cracked and they have a very good ratio of stiffness and weight. Energy consupmted during the composite failure is also taking part in the mitigation of the impact conseqences.

4.1.1 Basic theory

In the case of fibre composites the group can be devided into the long-fibre and short-fibre composites. Short-fibre composites can be produced easier for example by the injection moulding, but fibre directions can usually not be controlled. This work deals with the long-fibre composites that can be further devided into the unidirectional and multidirectional. Those composites usually consists of so called laminas - plies of the certain thickness that are mostly unidirectional or made of woven textile. Laminas are composed together under the specific angles to obtain the required material properties.

Unidirectional composites

In the basic analysis, unidirectional composite can be handled as transversally orthotropic material [12]. There exists the main anisotropy direction (direction of the fibres) and so called isotropy plane, that is perpendicular to the main direction. Properties in the isotropy plane are equal for all the directions.

It is often situation that not enough experiments examinating the elastic properties of the final composite can be realized. Therefore, calculation of those values from known

elastic parameters of fibres and matrix (usually provided by producer) must be carried out.

Elastic parameters of unidirectional composite According to [12] planar 2D lamina is described by 4 parameters:

E_{11} - elasticity modulus in the direction of the fibres,
E_{22} - elasticity modulus in the transversal direction,
ν_{12} - Poisson's ration in the plane of lamina,
G_{12} - shear modulus in the plane of lamina.

Following formulas are derived in detail in [12]:

$$E_{11} = V_f E_f + (1 - V_f) E_m, \tag{4.1}$$

$$E_{22} = \frac{E_m}{1 - V_f(1 - \frac{E_m}{E_f})}, \tag{4.2}$$

$$\nu_{12} = V_f \nu_f + (1 - V_f) \nu_m, \tag{4.3}$$

$$G_{12} = \frac{G_m}{1 - V_f(1 - \frac{G_m}{G_f})}. \tag{4.4}$$

Nevertheless, since such a material is expected to be modelled as three dimensional and material is orthotropic, 5 more parameters is needed:

E_{33} - elasticity modulus in the direction perpendicular to the plane of lamina,
ν_{23} - Poisson's ratio in the plane defined by transversal and perpendicular directions,
ν_{13} - Poisson's ratio in the plane defined by longitudinal and perpendicular directions,
G_{23} - shear modulus in the plane defined by transversal and perpendicular directions,
G_{13} - shear modulus in the plane defined by longitudinal and perpendicular directions.

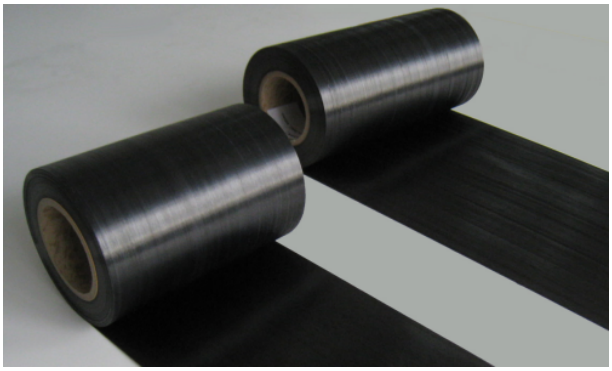

Figure 4.1: Reel of unidirectinal prepreg (presaturated fibres) [10].

Whereas the situation is simplified by relations

$$E_{22} = E_{33}, \tag{4.5}$$

$$G_{12} = G_{13}, \tag{4.6}$$

$$\nu_{12} = \nu_{13}, \tag{4.7}$$

and the remaining two parameters are estimated as [13]:

$$G_{23} = \frac{E_{22}}{(2(1+\nu_{23}))}, \tag{4.8}$$

$$\nu_{23} = \nu_m \frac{(1+\psi V_f)}{(1-\psi V_f)}, \tag{4.9}$$

where

$$\psi = \frac{(\frac{\nu_f}{\nu_m}-1)}{(\frac{\nu_f}{\nu_m}+1)}. \tag{4.10}$$

Laminates

The practicall useage of the unidirectional composites in the complex structures is a rare thing, although there are some exceptions [14]. Usually it is advantageous to produce composites in the form of laminates. These consist of so called laminas - layers of differently oriented fibres. Laminas can be unidirectional, biaxial or made of woven textile. In the case of unidirectional laminas, designer can decide about each direction and optimize the structure. Above that, it is necessary to know only the fiber and matrix elastic properties to model such a laminate with a good accuracy.

4.1.2 Composite failure during impacts

Failure of the long fibre composites and it's continuous damage is a complex field. There exist many failure criteria. The basic failure conditions expressed in Maximal stress and Maximal strain criterion are appropriate for the first approach because of incohesion of the particular stress components and it's influence on the composite failure. Criteria like Puck or Tsai-Wu interconnects the stress components into the equation. These criteria are called interactive. Nevertheless, it has been found out that the failure of the fibre composites offently consists of more failure modes that depend mainly on the loading. Therefore, so called "direct mode" criteria should be used in the more accurate approach of the damage initiation.

Hashin criterion One of the direct mode criteria is "Hashin damage initiation" introduced in 1980 for unidirectional composites [16]. This criterion considers four different damage initiation mechanisms: fiber tension, fiber compression, matrix tension, and matrix compression. An example of such a damage modes can be observed at Fig. 4.2. Hashin criterion is advantageous to use because of it's interactivity and sufficiently accurrate agreement with the experimental results, prooved e.g. in [15]. Furthermore, needed strength parameters are easy to measure or find and it is implemented in Abaqus solver.

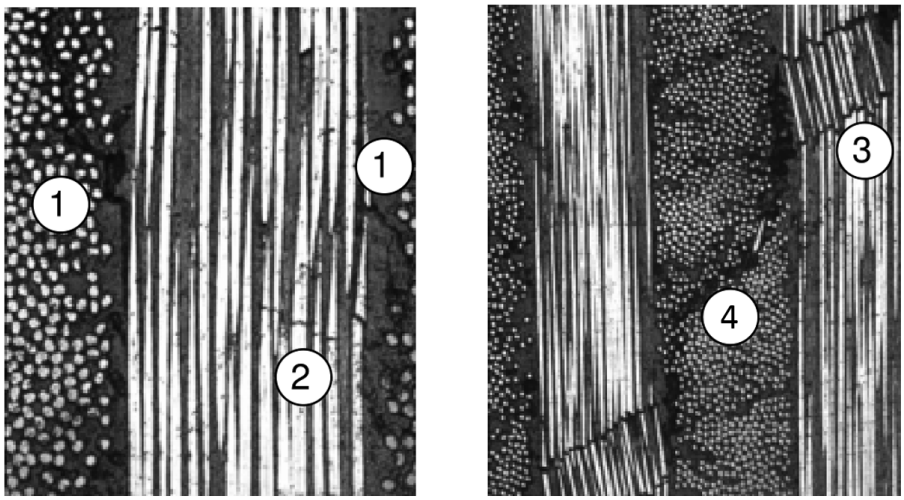

Figure 4.2: Example of the damage modes considered by Hashin criterion. 1 - matrix failure in tension, 2 - fibre failure in tension, 3 - fibre failure in compression, 4 - matrix failure in compression. [17]

The initiation criteria have the following general forms [16]:
Fiber tension $\overline{\sigma}_{11} \geqq 0$:

$$F_f^t = (\frac{\overline{\sigma}_{11}}{X^T})^2 + \alpha(\frac{\overline{\tau}_{12}}{S^L})^2. \tag{4.11}$$

Fiber compression $\overline{\sigma}_{11} < 0$:

$$F_f^c = (\frac{\overline{\sigma}_{11}}{X^C})^2. \tag{4.12}$$

Matrix tesnsion $\overline{\sigma}_{22} \geqq 0$:

$$F_m^t = (\frac{\overline{\sigma}_{22}}{Y^T})^2 + (\frac{\overline{\tau}_{12}}{S^L})^2. \tag{4.13}$$

Matrix compression $\overline{\sigma}_{22} < 0$:

$$F_m^c = (\frac{\overline{\sigma}_{22}}{2S^T})^2 + [(\frac{Y_C}{2S^T})^2 - 1]\frac{\overline{\sigma}_{22}}{Y_C}(\frac{\overline{\tau}_{12}}{S^L})^2. \tag{4.14}$$

In the above equations X^T denotes the longitudinal tensile strength, X^C the longitudinal compressive strength, Y^T the transverse tensile strength, Y^C the transverse compressive strength, S^L longitudinal shear strength, S^T the transverse shear strength.

4.1.3 Selected materials

Requirements for the "hard" helmet shell are not simple. Shell must be stiff to carry the shock loads into the liner. In the same time, shell should have a good ratio of weight and crashworthiness. Crashworthiness expresses an ability of the material to absorb the mechanical energy in it's damage process. Due to the high strength limits of the carbon fibres, carbon fibre reinforced plastics (CFRP's) exceed in crashworthiness [18]. Nevertheless, there are many factors that have influence on so called Specific energy absorption [kJ/kg] defined in [19]. Three factors are crucial - the material of the matrix, fibre directions and the cooling process. Table 4.1 shows an examples of the material crashworthiness measured by quasi-static compressive tests of tube-shaped samples.

Fibre	Matrix	Specifications	Specific energy absorption [kJ/kg]
Carbon fiber	Epoxy	Fiber architecture +- 45°	53
Glass fiber	Epoxy	Fiber architecture 0/90°	60
Kevlar fiber	Epoxy	Fiber architecture +- 45°	63
Carbon fiber	PEEK	Fiber architecture +- 30°	127
Carbon fiber	PEEK	Fiber arch. 0°, slowly cooled	197
Carbon fiber	PEEK	Fiber arch. 0°, rapidly cooled	226

Table 4.1: Examples of material Specific energy absorption according to [19].

PEEK - polyetheretherketone is an organic thermoplastic polymer. Mechanical properties of this material (tensile strength up to 100 MPa) exceeds the epoxy resin matrices while being lighter (1320 kg/m^3). Besides good crashworthiness, carbon/PEEK composite can be repeatedly thermally treated - the small matrix cracks can be fixed. Thus, the carbon fibre/PEEK matrix composite can be reccomended to be used in the helmet design.

Unfortunatelly, one of the disadvantages of such a composite is it's availability. Even when available, obtaining of all material parameters that are needed is a long and labouring proccess exceeding the scope of this work. Therefore, the carbon fibre/epoxy resin composite with known material parameters (Tab. 4.2) was considered in the following helmet design. Elastic parameters were calculated using equations 4.1-4.10. Strength parameters were estimated from the literature ([20], [21], [13]) considering volume ratio of fibres 52%. Energetic parameters needed for the progressive damage [23] model are:

G_{ft}^C - energy dissipated during damage of the fiber in tension [17],
G_{fc}^C - energy dissipated during damage of the fiber in compression [17],
G_{mt}^C - energy dissipated during damage of the matrix in tension [24],
G_{mc}^C - energy dissipated during damage of the matrix in compression [24].

E_{11} [GPa]	225.8	X^T [MPa]	1400
E_{22} [GPa]	4.3	X^C [MPa]	366
E_{33} [GPa]	4.3	Y^T [MPa]	21
G_{13} [GPa]	2.4	Y^C [MPa]	92
G_{23} [GPa]	2.4	S^L [MPa]	42
G_{12} [GPa]	1.6	S^T [MPa]	42
ν_{12} [-]	0.3755	G^C_{ft} [kJ/m^2]	91.6
ν_{23} [-]	0.3747	G^C_{fc} [kJ/m^2]	79.9
ν_{31} [-]	0.3755	G^C_{mt} [kJ/m^2]	1.4
Density	1448 [kg/m^3]	G^C_{mc} [kJ/m^2]	1.4

Table 4.2: Elastic, strength and energetic parameters of considered carbon composite.

4.2 Liner

As mentioned in the previous chapters, liner is probably the most important part of the helmet. There exist helmets without any liners but they are primarily resistant only against the penetration by other objects. Main purpose of the liner is to absorb as much mechanical energy of the impact as possible and reduce the decceleration and forces transferred to the user's head that could cause the brain injuries.

4.2.1 D3O

D3O is a trademark of material that has been developed and produced by british company D3O since 2006. The company is focused on using D3O in the protective elements for athletes, motorsports and recently also for the military sector. D3O is usually being used in the various forms of pads such as knee, elbow, ankle or spinal (Fig. 4.4). Thanks to it's compliance, even big protectors can be produced as a single part, whereas plastic protectors must be made of several parts.

Figure 4.3: D3O in the original form before mixing with polymer [25].

Basic properties

From the technical point of view, D3O is a viscoelastic compound of dilatant non-newtonian fluid and polymer (Fig. 4.3). Dilatant fluids are characterized by raising it's apparent stiffness with the raising deformation speed. This phenomenon is called strain-rate effect. One of the best known dilatant fluids are starch or toothpaste. One of the main problems when using these materials to transmit the loading is their shape instability. When speaking about D3O, shape stability is ensured by the elastic polymer. Searching for a stable compound was one of the most difficult problems that had to be solved before launching D3O on the market.

Figure 4.4: Various protection pads made of D3O [26].

Casts made of D3O offently exists in the several variants of the different density and protection level. One of the main advantages of the protective elements made of D3O is their formability and flexibility whereas it solidifies only in the case of the impact and distribute the impact load into the wider surface and turning the impact energy into the heat (D3O shows no plastic deformation).

4.2.2 EPS

One of the most common materials of the helmet liner is expanded polystyrene (EPS) [27]. Polystyrene is a synthetic aromatic polymer made by polymerization of the styrene monomers. It is a rigid substance in its original form. EPS is a foamed version very famous for it's low weight, low price and high protection factor. Therefore, it is being used mainly in the packaging industry but also as a thermoisolation material or material of the various disposable food containers.

Basic properties

EPS can be produced in the many different densities (different porosities) and energy absorption capabilities. Density of EPS that was used as a protective liner in the examined helmet on Fig. 2.7 is 100 kg/m3. Due to it's chemical property and microstructure (Fig. 4.6), damage mechanism of expanded polystyrene is mainly cracking of the cell walls on the microscopic level. However, this behavior can be observed as the plastic deformation on the macroscopic level. Therefore, it can be describe by elasto-plastic theories as mentioned further.

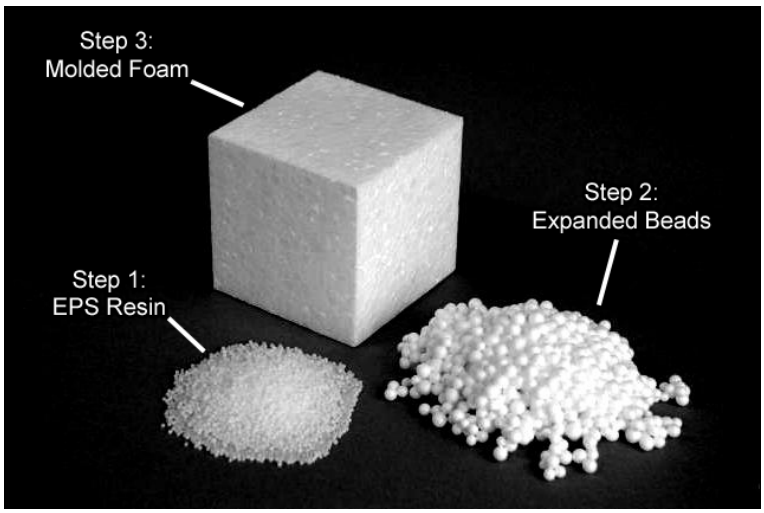

Figure 4.5: Expanded PolyStyrene [28].

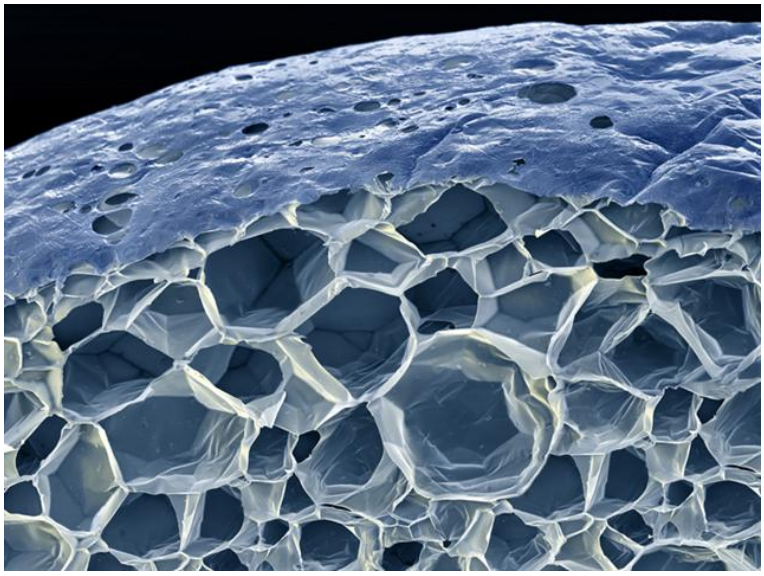

Figure 4.6: Microstructure of the EPS cell. [28]

4.2.3 Experiments

Two types of experiments were performed with D3O and EPS in order to provide the data needed for the indentification of the elastic, viscoelastic and plastic parameters needed for the numerical models. Samples of simple geometry that were cut out of the intact knee protector (D3O) and bicycle helmet (EPS) can be seen for example on Figs. 4.7 and were used for the both experiments.

Compression test Compression test was based on the exposure of the sample to the constant value of the displacement in the particular time whereas the force response was measured. The reverse form of this test is called 'Creep test' and in that case the sample is exposured to the constant value of stress. Testing machine Zwick-Roell Z050 was used for the compression relaxation tests. After placing the sample between compression clamps

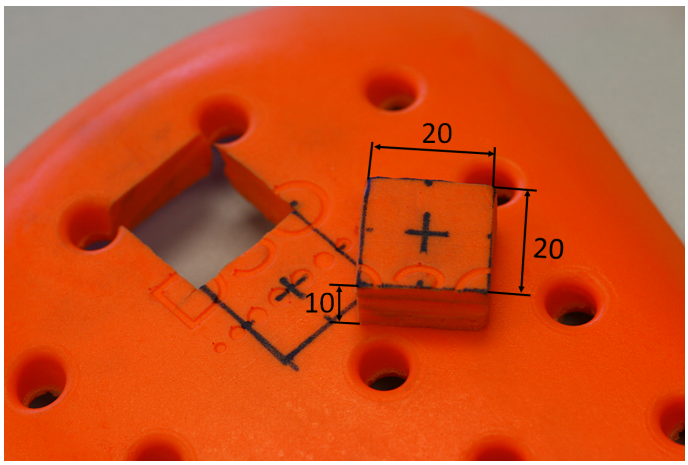

Figure 4.7: D3O sample dimensions [mm].

(Fig. 4.8) it was partially preloaded with the low force of 10 N and then loaded to the particular value of the strain. The strain was hold over the time t and then removed with the following relaxation pause. This cycle was repeated two times. The highest loading velocity that could be reached on Zwick-Roell Z050 was set in the experiments. It caused that the predesrcibed displacement was exceeded (each sample was exposed to a little different displacement and it also caused the negative displacement visible on Fig. 4.11). Tab. 4.3 and Tab. 4.4 sum up the details of the measurement for the particular samples.

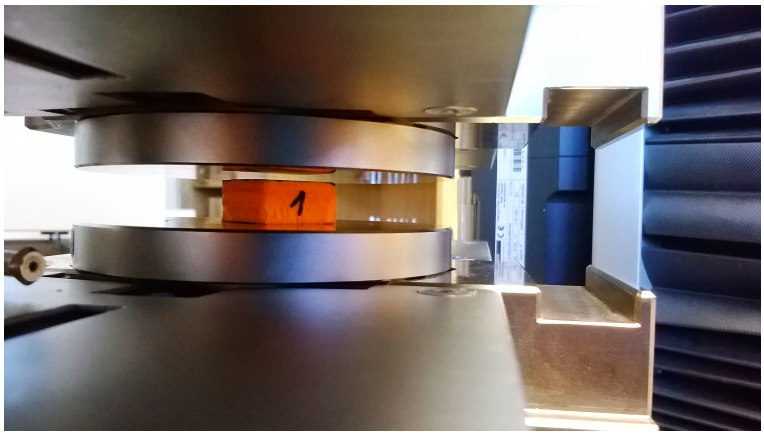

Figure 4.8: D3O sample ready in the clamps for the compression test.

Sample	Deformation	Displacement [mm]	Velocity [mm/s]	Preload [N]	Relaxation time [s]
1	0.36	3.6	10	10	60
2	0.36	3.6	10	10	60
1	0.33	3.3	5	10	60

Table 4.3: Summation of D3O compression measurement.

Sample	Deformation	Displacement [mm]	Velocity [mm/s]	Preload [N]	Relaxation [s]
1	0.12	1.2	10	10	60
2	0.20	2.0	10	10	60
3	0.22	2.2	10	10	60
4	0.34	6.7	10	10	60

Table 4.4: Summation of EPS compression measurement.

The compression test gave the important information about the material behavior during several loading cycles and about the mechanical energy transformation. As can be seen on Fig. 4.11, material shown no plastic deformation in the case of D3O even when exposed to approx. 30 % strain.

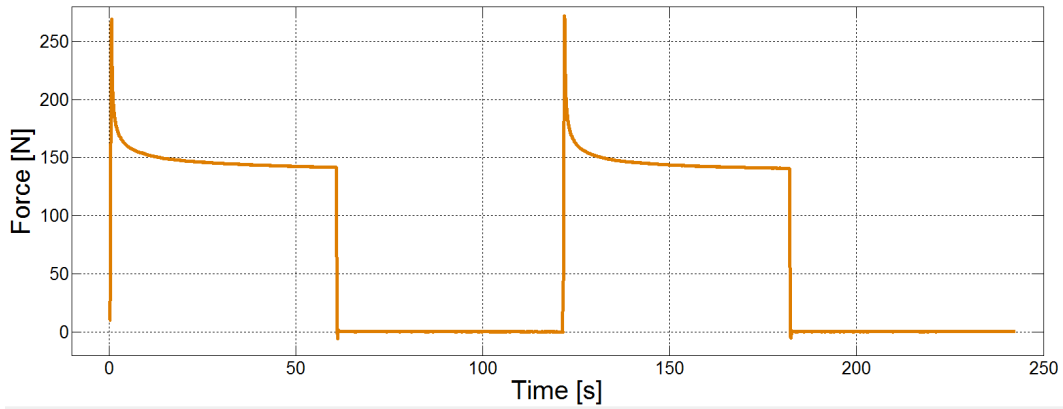

Figure 4.9: Force-time curve measured in the compression relaxation test of D3O.

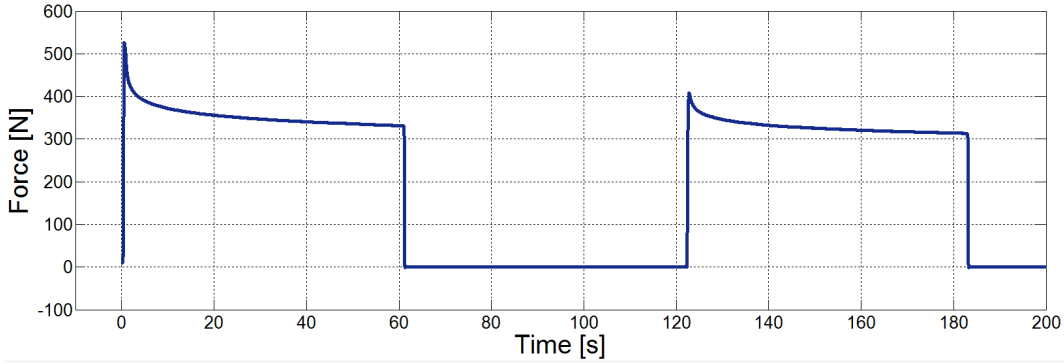

Figure 4.10: Force-time curve measured in the compression relaxation test of EPS.

Practically all mechanical energy is transformed into the heat. Therefore, it can be confirmed that D3O material is very suitable for the repeatable loadings for example impacts. It can also be observed from Fig. 4.9 that viscoelastic behavior of D3O is significant because the reaction force dropped to the nearly 50% in a minute. In case of EPS, relaxation tests were carried out in order to prove the material behavior (plastic deformation) that can be observed for example on hystheresis loop on Fig. 4.12.

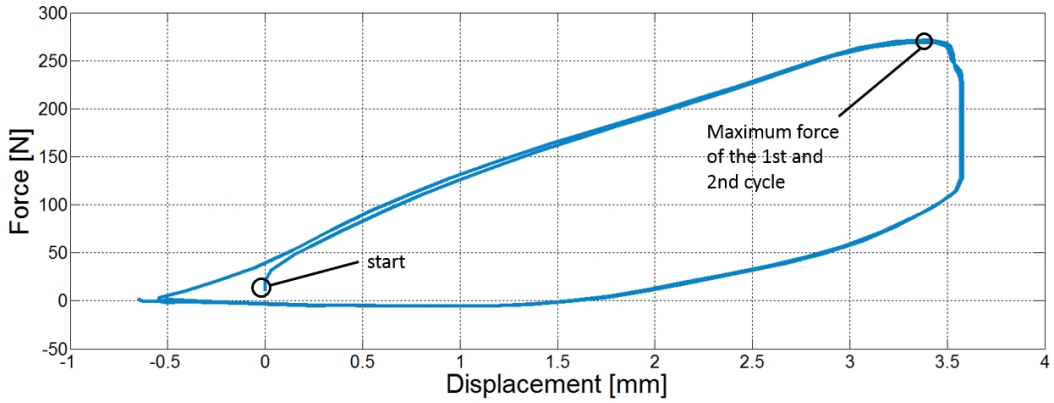

Figure 4.11: Force-displacement curve (hystheresis loops) measured in the compression relaxation test of D3O.

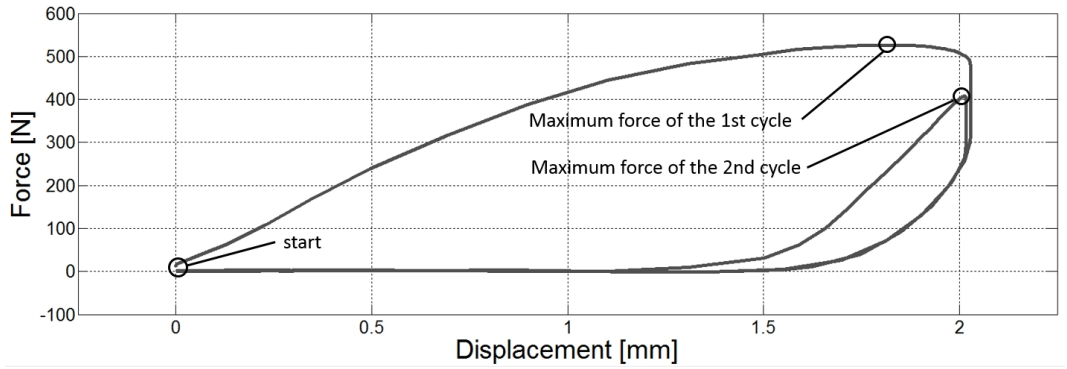

Figure 4.12: Force-displacement curve (hystheresis loops) measured in the compression relaxation test of EPS.

Impact test Impact tests (Fig. 4.16 - 4.35) were performed using the dropping machine constructued in the Department of mechanics. It contains of the dropping rail that enables to use more types of the dropping weigth (see Fig. 4.13). Force sensor is placed between the tip and the rest of the weigth (see Fig. 4.14).

Two types of impactors were used to measure the impact response. The experiments with the semispherical impactor were captured by hishspeed camera in order to identify the basic behavior (example can be seen on Fig. 4.15). Experiments with the flat impactor were used to measure the response that was further used in te optimization algorithm in order to identify seven viscoelastic parameters in case of D3O and seven elasto-plastic parameters in case of EPS.

Impact test were performed for the various impact energies that are summed up in Tab. 4.5 and 4.6 together with the maximal force peaks registered.

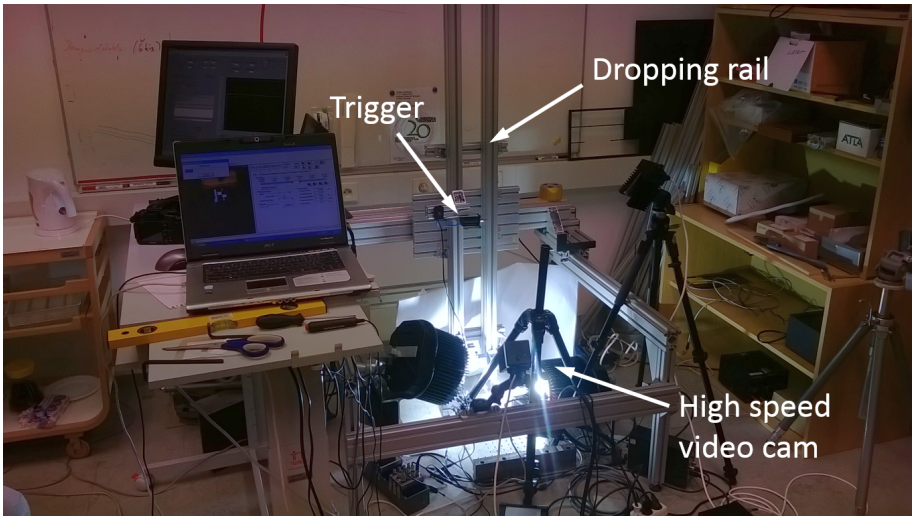

Figure 4.13: Dropping device used for the impact tests.

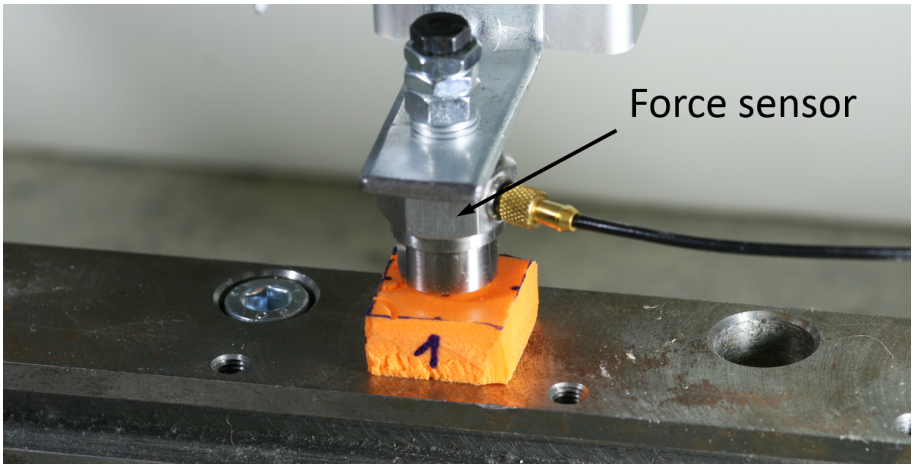

Figure 4.14: Semispherical impactor with the force sensor.

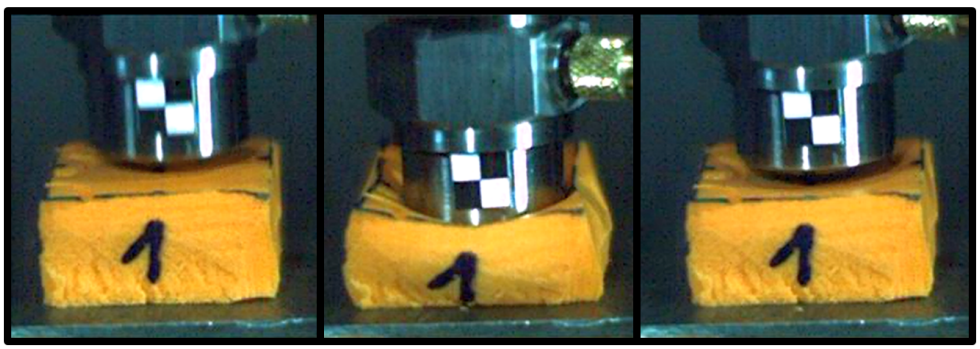

Figure 4.15: D3O impact behavior captured by highspeed camera for the impact velocity of 4,5 m/s.

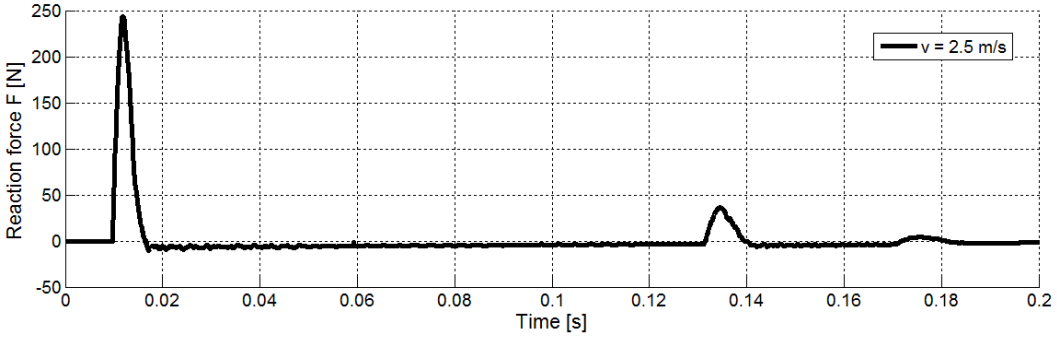

Figure 4.16: D3O impact behavior, sample 1, semispherical impactor, velocity 2,5 m/s.

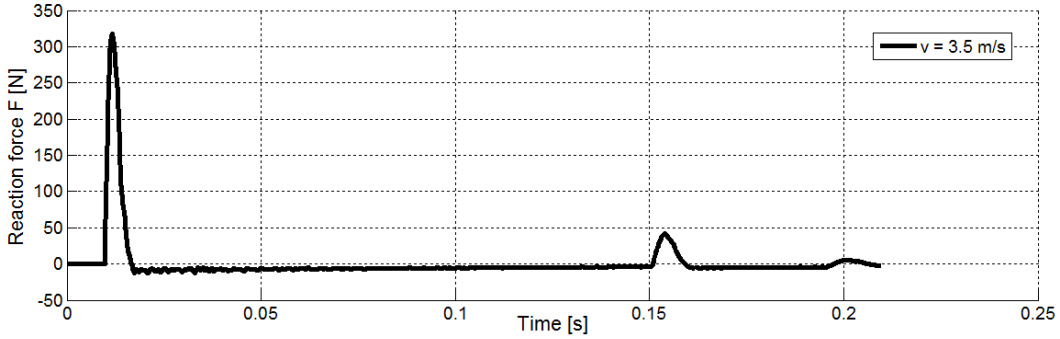

Figure 4.17: D3O impact behavior, sample 1, semispherical impactor, velocity 3,5 m/s.

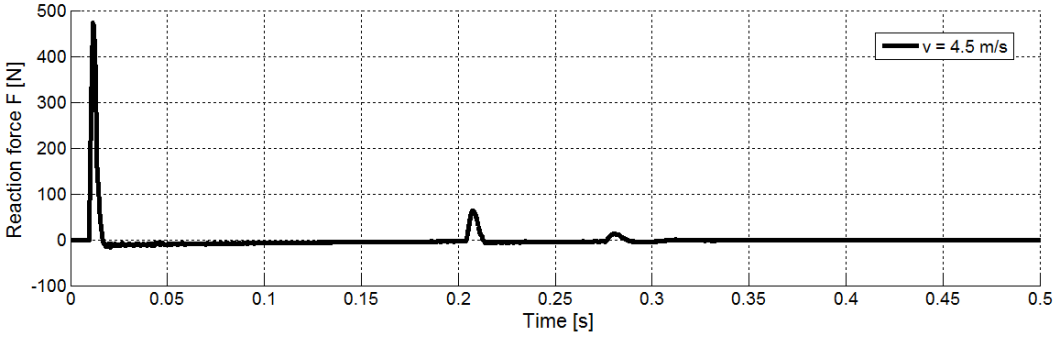

Figure 4.18: D3O impact behavior, sample 1, semispherical impactor, velocity 4,5 m/s.

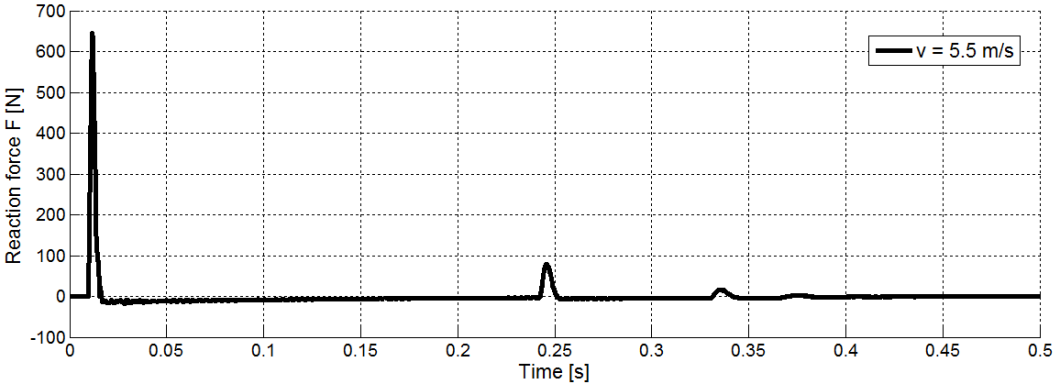

Figure 4.19: D3O impact behavior, sample 1, semispherical impactor, velocity 5,5 m/s.

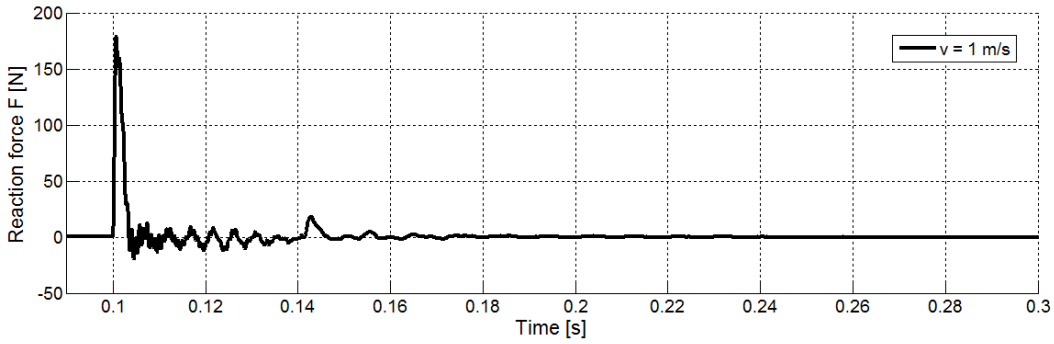

Figure 4.20: D3O impact behavior, sample 1, flat impactor, velocity 1 m/s.

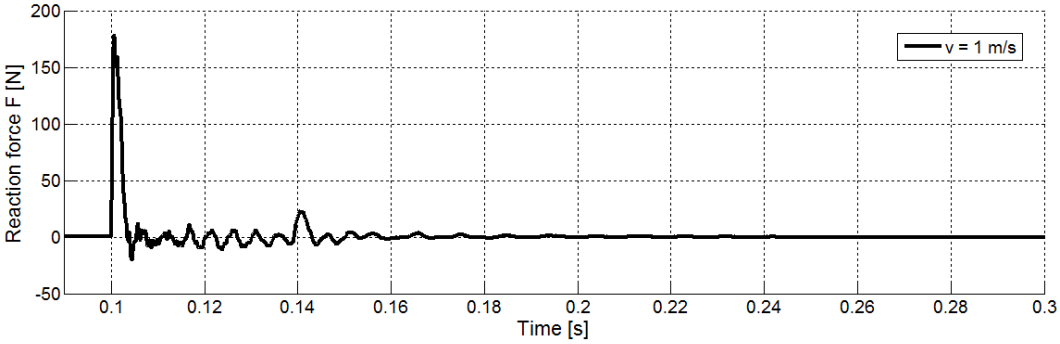

Figure 4.21: D3O impact behavior, sample 2, flat impactor, velocity 1 m/s.

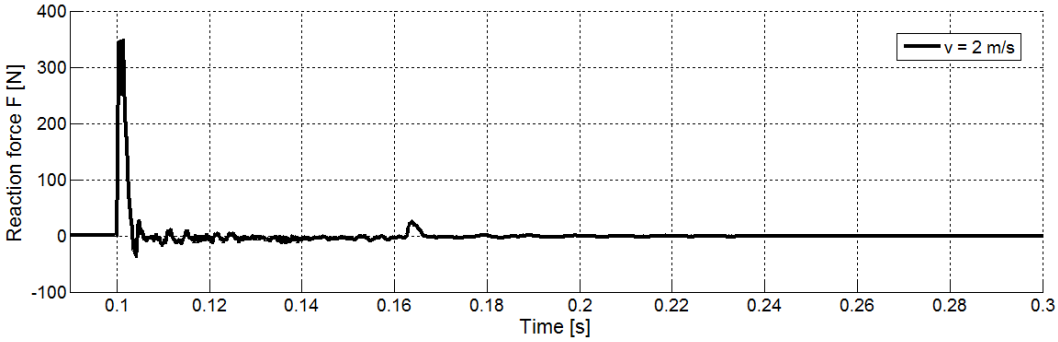

Figure 4.22: D3O impact behavior, sample 1, flat impactor, velocity 2 m/s.

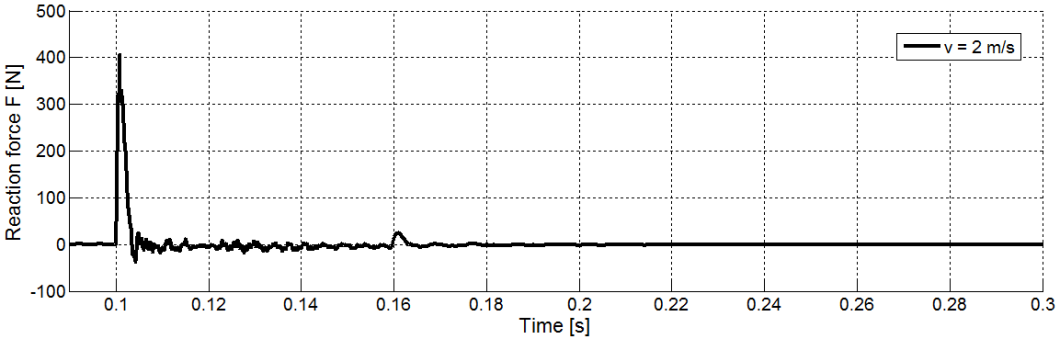

Figure 4.23: D3O impact behavior, sample 2, flat impactor, velocity 2 m/s.

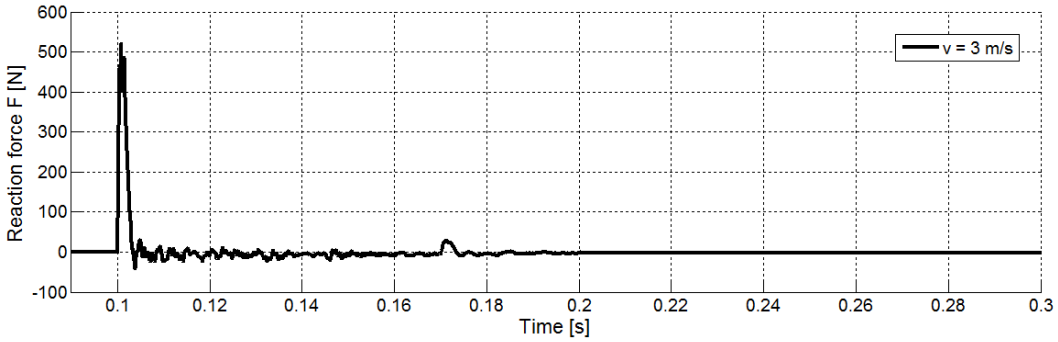

Figure 4.24: D3O impact behavior, sample 1, flat impactor, velocity 3 m/s.

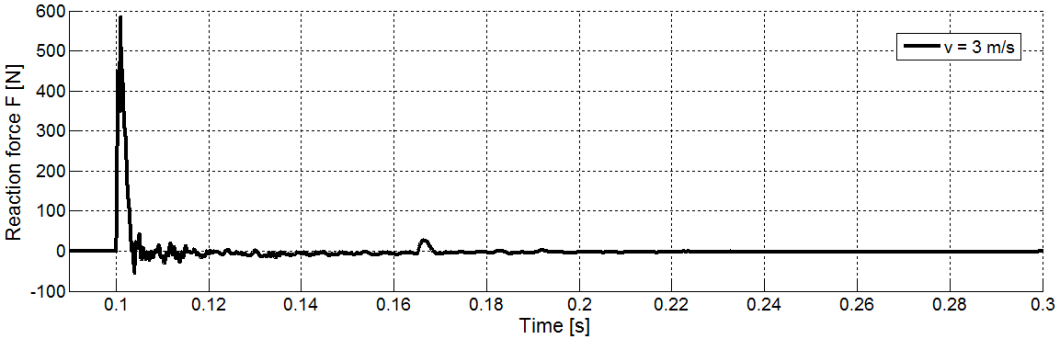

Figure 4.25: D3O impact behavior, sample 2, flat impactor, velocity 3 m/s.

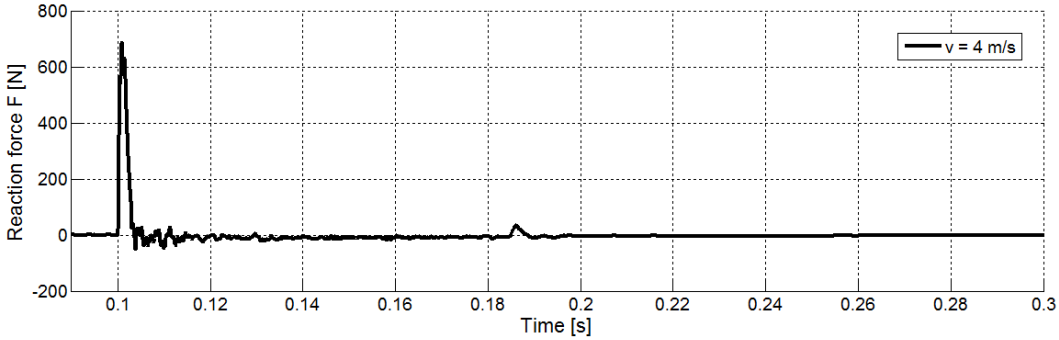

Figure 4.26: D3O impact behavior, sample 1, flat impactor, velocity 4 m/s.

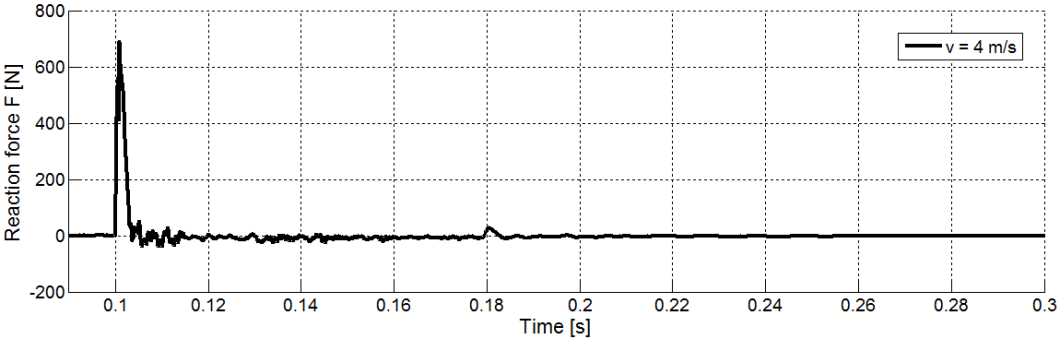

Figure 4.27: D3O impact behavior, sample 2, flat impactor, velocity 4 m/s.

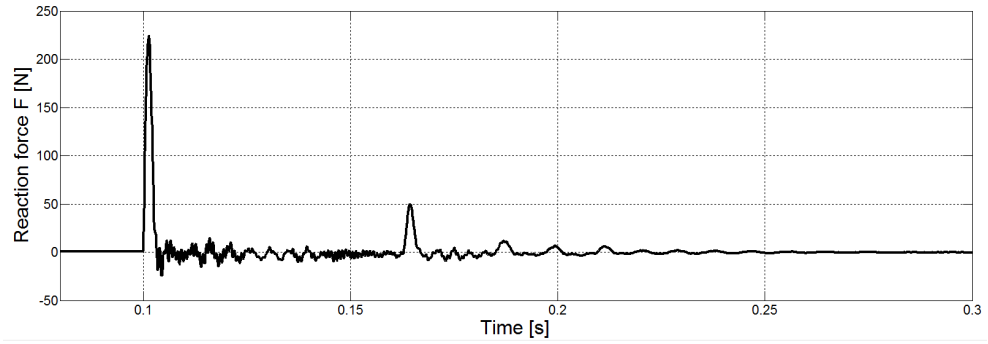

Figure 4.28: EPS impact behavior, sample 1, flat impactor, velocity 1 m/s.

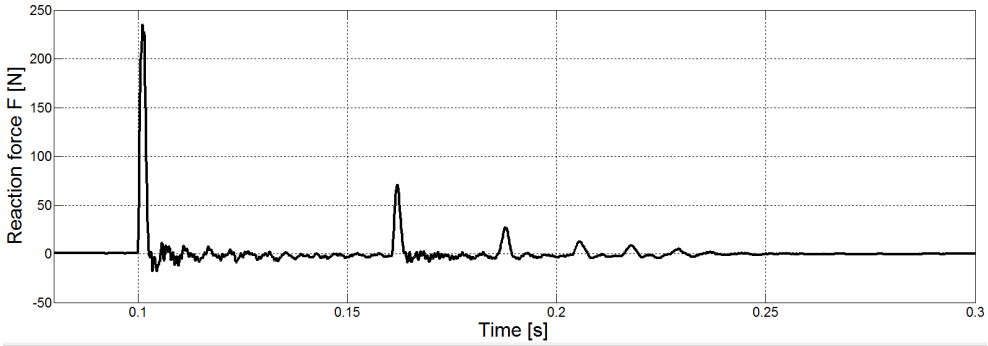

Figure 4.29: EPS impact behavior, sample 2, flat impactor, velocity 1 m/s.

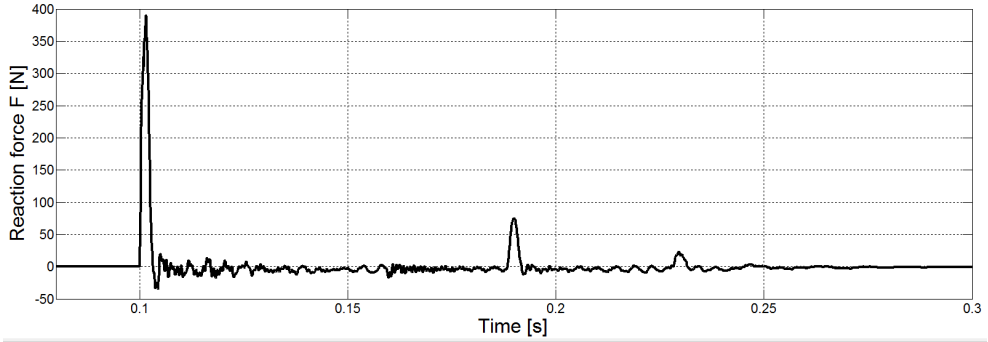

Figure 4.30: EPS impact behavior, sample 3, flat impactor, velocity 2 m/s.

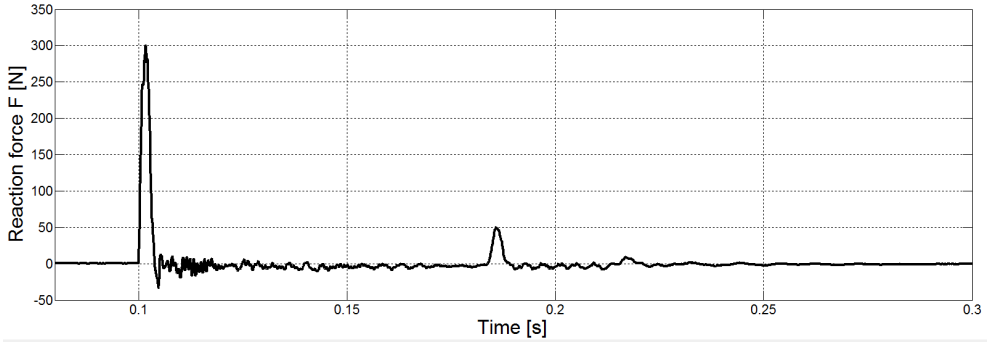

Figure 4.31: EPS impact behavior, sample 4, flat impactor, velocity 2 m/s.

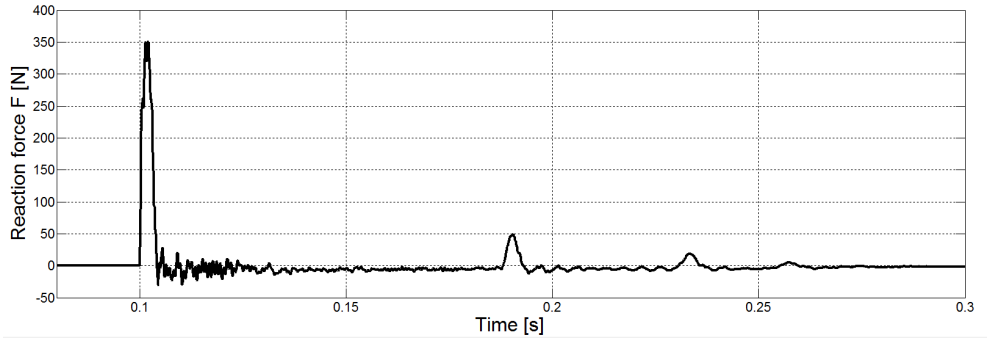

Figure 4.32: EPS impact behavior, sample 5, flat impactor, velocity 3 m/s.

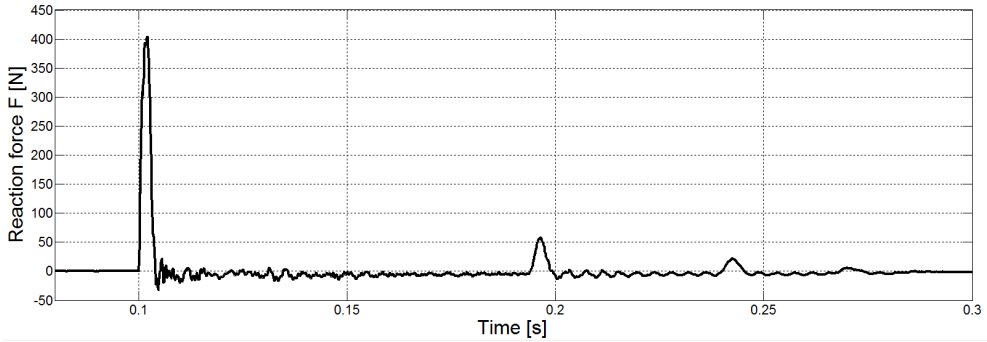

Figure 4.33: EPS impact behavior, sample 6, flat impactor, velocity 3 m/s.

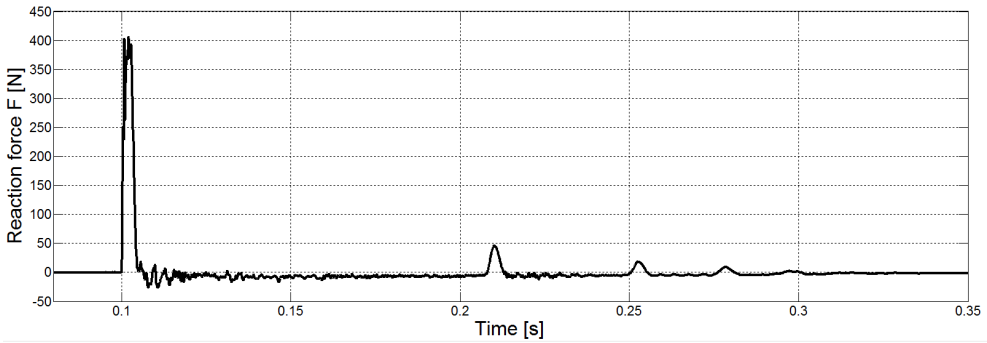

Figure 4.34: EPS impact behavior, sample 7, flat impactor, velocity 4 m/s.

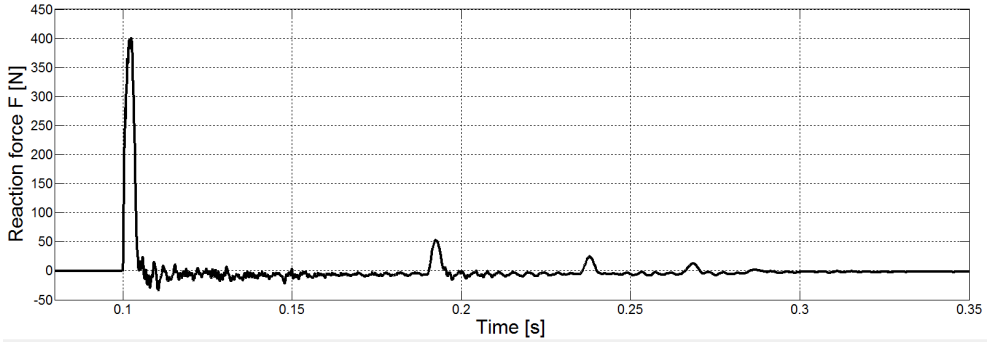

Figure 4.35: EPS impact behavior, sample 8, flat impactor, velocity 4 m/s.

Sample	Impact velocity [m/s]	Impactor type	Impactor weight [g]	Impact energy [J]	Max. force [N]
1	2,5	Semispherical	246	0,77	245
1	3,5	Semispherical	246	1,50	321
1	4,5	Semispherical	246	2,49	478
1	5,5	Semispherical	246	3,72	646
1	1	Flat	350	0,18	175
2	1	Flat	350	0,18	176
1	2	Flat	350	0,70	348
2	2	Flat	350	0,70	408
1	3	Flat	350	1,58	510
2	3	Flat	350	1,58	585
1	4	Flat	350	2,80	684
2	4	Flat	350	2,80	691

Table 4.5: Summation of D3O impact measurement.

Sample	Impact velocity [m/s]	Impactor type	Impactor weight [g]	Impact energy [J]	Max. force [N]
1	1	Flat	350	0,18	225
2	1	Flat	350	0,18	240
3	2	Flat	350	0,70	390
4	2	Flat	350	0,70	305
5	3	Flat	350	1,58	350
6	3	Flat	350	1,58	405
7	4	Flat	350	2,80	408
8	4	Flat	350	2,80	405

Table 4.6: Summation of EPS impact measurement.

4.2.4 Material models

Viskoelasticity of D3O

As mentioned before, D3O has a significant strain-rate viscoelastic behavior. It means that material is capable to transform the mechanical energy of deformation into the thermal energy due to the internal material friction. There are several mathematical models decribing this behavior.

Zener model One dimensional "Zener" model was chosen for the first approach (relaxation).

Zener viscoelastic model consists of two branches - serial connected spring and damper and paralelly connected elastic spring model (see Fig. 4.36). Mechanical properties are determined by three parameters - elastic modulus E_∞, E_s and viskosity η.

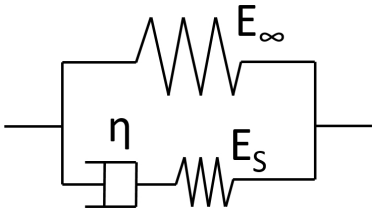

Figure 4.36: Zener model.

Therefore Zener model is also called 'Three-parametrical model'. According to [22] stress τ transfered by viscoelastic element is

$$\begin{aligned} \tau &= E_\infty e + \sigma_\mathrm{s}, && (4.15)\\ \sigma_\mathrm{s} &= E_\mathrm{s} e_\mathrm{s} = \eta \dot{e}_\mathrm{d}, && (4.16)\\ e &= e_s + e_d, && (4.17) \end{aligned}$$

where e is total strain, e_s and e_d are strains of serial connected spring and damper. Expressing stress σ_s in serial branch we can obtain

$$\tau = (E_\infty + E_\mathrm{s})e + E_\mathrm{s} e_\mathrm{d} = E_0 - q = \sigma - q, \quad (4.18)$$

where $E_0 = E_\infty + E_s$ is stiffness of elastic response $\sigma = E_0 e$ and q is a parameter having a dimension of stress. Adjusting (4.16) evolutionary equation is obtained

$$\begin{aligned} \eta \dot{e}_\mathrm{d} &= E_\mathrm{s}(e - e_\mathrm{d}), && (4.19)\\ \dot{e}_d + \frac{E_s}{\eta} e_d &= \frac{E_s}{\eta} e, && (4.20) \end{aligned}$$

that can be adjusted by newly introduced relaxation coefficient γ and relaxation time T_e:

$$E_s = \gamma E_0, 0 < \gamma < 1, \tag{4.21}$$
$$T_e = \frac{\eta}{E_s}. \tag{4.22}$$

Using (4.20) evolutionary equation is transfromed into

$$\dot{q} + \frac{1}{T_e} q = \frac{\gamma}{T_e} \sigma(e), \tag{4.23}$$

whereas appliyng

$$\sigma(e) = E_0 e, \tag{4.24}$$
$$\tau(t) = \sigma(t) - q(t), \tag{4.25}$$
$$E_0 = E_\infty + E_s, \tag{4.26}$$
$$\gamma = \frac{E_s}{E_0}, \tag{4.27}$$
$$E_\infty = (1-\gamma) E_0, \tag{4.28}$$

and solution is searched in interval

$$i) t \in [0, T], q(0) = 0, \tag{4.29}$$
$$ii) t \in [-\infty, T], \lim_{t \to -\infty} q(t) = 0. \tag{4.30}$$

Besides zero initial condition for q we consider $e(0) = 0$.

When substituing $q = \sigma - \tau$ into (4.23) we obtain diferential equation, which gives relation between strain and viscoelastic stress in the element when solved.

$$\dot{\sigma} + \frac{(1-\gamma)}{T_e} \sigma = \dot{\tau} + \frac{1}{T_e} \tau, \tag{4.31}$$
$$\dot{\tau} + \frac{1}{T_e} \tau = \dot{\sigma} + \frac{1}{T_\tau}, \tag{4.32}$$
$$T_\tau = \frac{T_e}{(1-\gamma)}. \tag{4.33}$$

If elastic response σ(t) for $t \in [0, T]$ is known, (4.32) can be solved :

$$\tau(t) = \tau(0) exp\{-\frac{1}{T_e}\} + \frac{T_e}{T_\tau} \left[exp\{\frac{s-t}{T_e}\} \sigma(s) \right]_0^t \tag{4.34}$$
$$+ \left(1 - \frac{T_e}{T_\tau}\right) \int_0^t exp\{\frac{s-t}{T_e}\} \frac{d}{ds} \sigma(s) ds. \tag{4.35}$$
$$\tag{4.36}$$

If we further consider unloaded initial state $\tau(0) = 0$ without initial strain, that means $\sigma(0) = 0$, relaxation equation is obtained:

$$\tau(t) = (1-\gamma)\sigma(t) + \gamma \int_0^t exp\{\frac{s-t}{T_e}\}\frac{d}{ds}\sigma(s)ds. \tag{4.37}$$

Because equation can be universally used even for non-zero initial conditions, it can be used for steady state that is the main part of the compression experiment. Step function that sets constant strain for $t < 0$ is used. Thus, viscoelastic stress for relaxing 1D element is

$$\tau(t) = \overline{\sigma} - \overline{\sigma}\gamma\left(1 - exp\{\frac{s-t}{T_e}\}\right), \tag{4.38}$$

$$\overline{\sigma} = E_0\overline{e}. \tag{4.39}$$

Prony series It was very soon found that one dimensional model will not suit all the requirements of the final helmet model such as 3D loading. Thus, viscoelasticity model described by so called Prony series [23] was chosen to be used. Advantages are full implementation Abaqus solver and proprocessor and possibility to choose appropriate number of parameters.

Those parameters are:

$\overline{g}_i^P$...shear relaxation modulus ratio,
k_i^P...bulk relaxation modulus ratio,
τ_i...relaxation time.

Since D3O was considered as incompressible, k_i^P was set to zero. Abaqus assumes that the viscoelastic bahavior is defined by Prony series expansion of the dimensionless relaxation modulus

$$G_R(t) = 1 - \sum_{i=1}^{N}\overline{g}_i^P(1 - e^{-t/\tau_i}), \tag{4.40}$$

where N is the number of elements of the series that can be chosen.

Plasticity of EPS

To affect the elasto-plastic behavior of EPS, standard elastic model combined with crushable foam model implemented in Abaqus was used. According to [23] crushable foam model requires two parameters:

$$k = \frac{\sigma_c^0}{p_c^0}, \tag{4.41}$$

where k is the yield stress ratio for compressive loading, σ_c^0 is the initial yield stress in uniaxial compression and p_c^0 is the initial yield stress in hydrostatic compression and

$$k_t = \frac{p_t}{p_c^0}, \tag{4.42}$$

where k_t is the yield stress ratio for the hydrostatic loading and p_t is the yield stress in the hydrostatic tension. As reccomended in [23] k_t parameter has no significant influenece in the compressive loading therefore it was set to 0.05. It would require complex and expensive tests to obtain p_c^0 experimentally. Therefore, it was identified with the other parameters.

Platic hardening of EPS is defined by the nonlinear plastic stress-strain curve. Example of such a curve can be seen on Fig. 4.37.

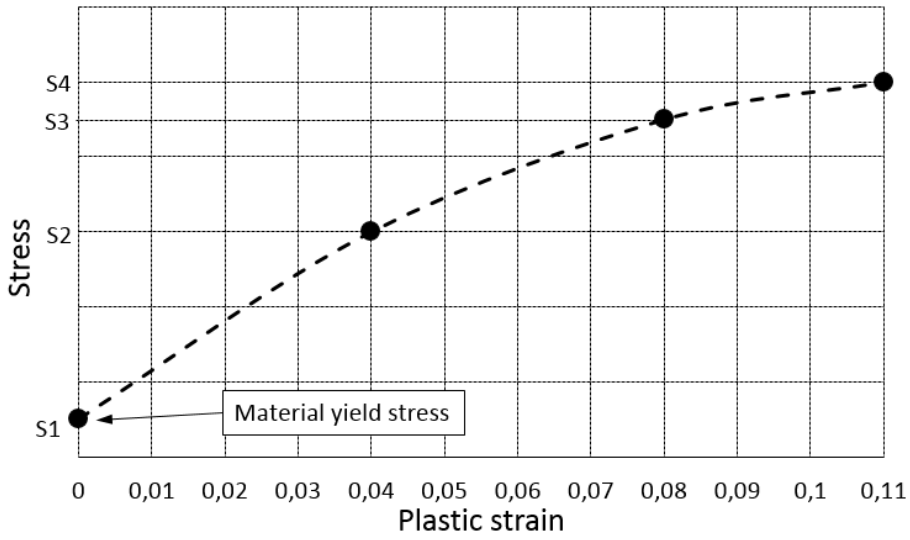

Figure 4.37: Example of a plastic curve.

4.2.5 Identification

Combination of the various software tools was used for the identification of the material parameters. Algorithm diagram can be observed on Fig. 4.38. Since the number of searched parameters was seven at maximum, constrained gradient algorithm was used to control the optimization process in all cases. Nature based stochastical algorithms are

recomended for significantly higher number of parameters and objective functions with lot of local minimizators.

In the case of unidimensional Zener model, stress (4.38) was recalculated into the force in each time point using the initial sample section surface. In the case of threedimensional FE models, the force was taken directly from the particular node. Then it was compared with the response obtained in the experiment that gives the objective function of the optimization process:

$$S = \sum_{i=1}^{n} (F_i^{exp} - F_i^{mod})^2. \tag{4.43}$$

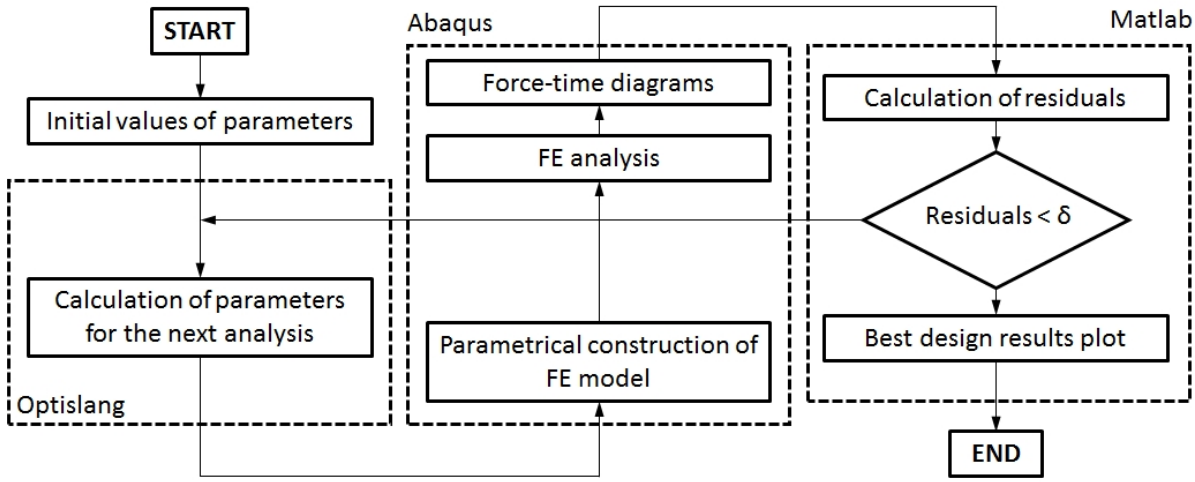

Figure 4.38: Identification algorithm diagram.

1D Zener model

Objective function had three input parameters of Zener model. Algorithm "Fminserach - unconstrained nonlinear minimization" from Matlab optimization toolbox was used to find the function minimum. It is a minimization without any constraints on the whole interval of the real numbers. Hand-found close solution was used as the starting vector. Fig. 4.39 shows the comparison of the experimental response and model driven by the optimized parameters. Identification of the parameters of Zener model stands out of the algorithm diagram on Fig. 4.38 since it was completely run in Matlab. The identified parameters are sum up in Tab. 4.7.

E_∞	1.604+e6 [MPa]
E_s	0.916+e6 [MPa]
η	1.618+e6 [MPa]

Table 4.7: Identified viscoelastic parameters of Zener model.

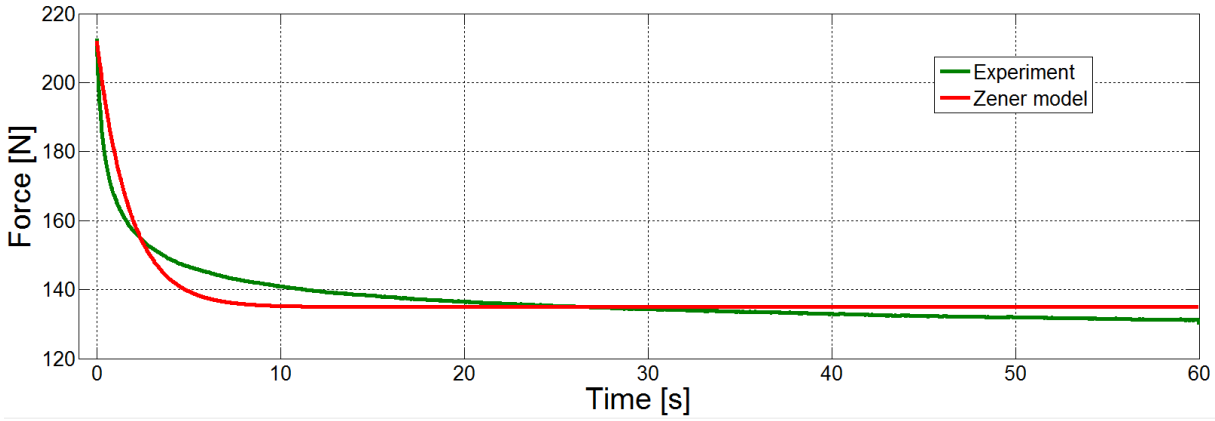

Figure 4.39: Comparison of the experimental relaxation D30 behavior and analytical Zener model with optimized parameters.

3D Prony series defined model

The identification algorithm (Fig. 4.38) was used to find seven viscoelastic parameters E^{d3o}, g_1, g_2, g_3, τ_1, τ_2, τ_3. Value of Poisson's ratio ν^{d3o} was determined by the optical measurement of the compression tests. Experimental and FE model response was devided into the same number of time increments, therefore, the residuals could be easily computed in all time points in the same way as in (4.43). That gives the objective function and constrained gradient minimization was used to find the minimum.

Relaxation It was supposed in advance that parameters in the compression and impact test will differ. The main reason is the strain-rate dependency. Nevertheless, identification of viscoelastic parameters from the compression test was important because it provided starting values for the identification of the parameters for the impact models. The example of comparison of the experimental values and FE model with identified parameters can be observed on Figs. 4.40 and 4.41.

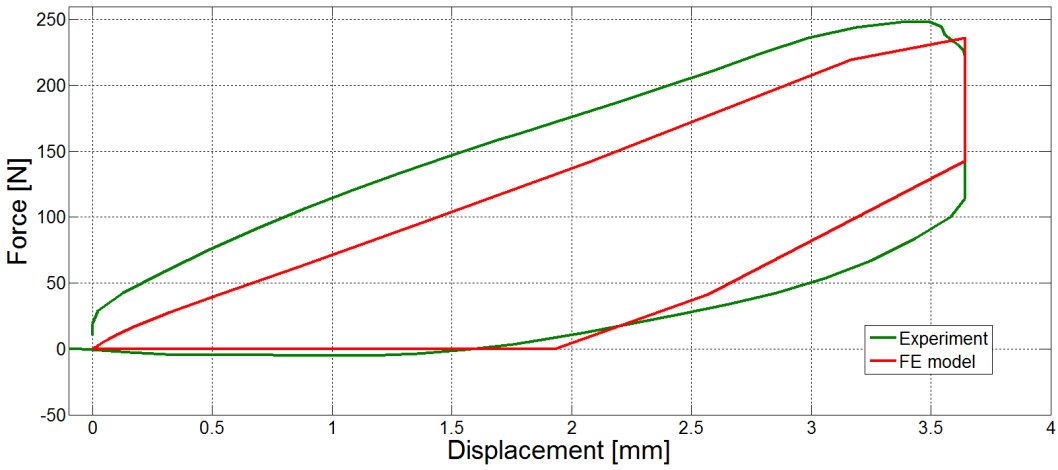

Figure 4.40: Comparison of experimental and FE model behavior of D3O in the compression, hystheresis loop, one cycle, sample 1.

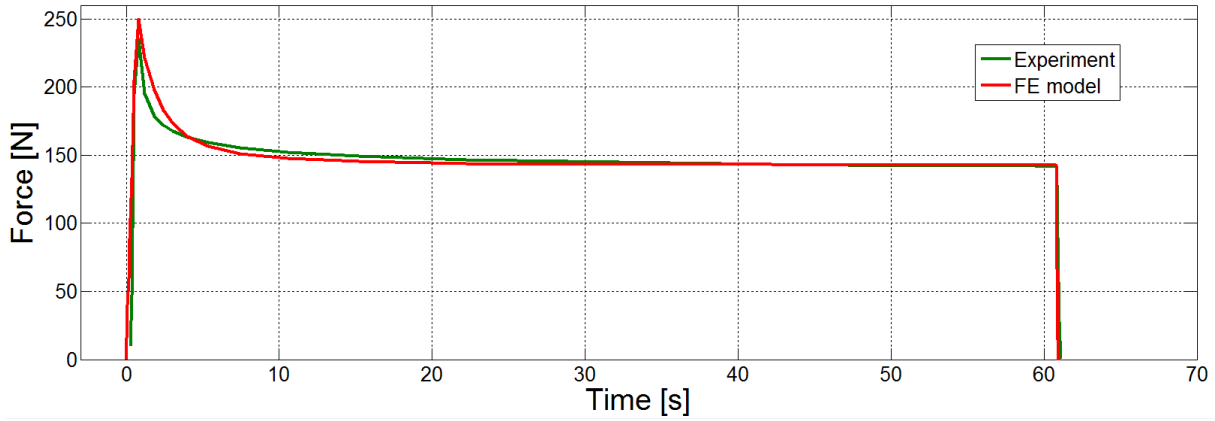

Figure 4.41: Comparison of experimental and FE model relaxation behavior of D3O in the compression, one cycle, sample 1.

Impact Data from the impact tests with the flat impactor were used for the identification of the viscoelastic parameters. Figs. 4.42 - 4.45 sum up each D3O impact experiment compared with FE model. Red line marked as "Parameters fit" represents FE model with parameters identified for the particular sample. It is also compared with the parameters identified for the other samples and velocities and then used in the model of the particular sample.

It can be observed from the figures that models with the averaged parameters are not very accurate in the beginning of the impact nor when the impactor is leaving for the first time. Nevertheless, the maximum peak of the force agrees. Therefore, fucntions determining ralatio between the viscoelastic parameters and the impact energy was defined.

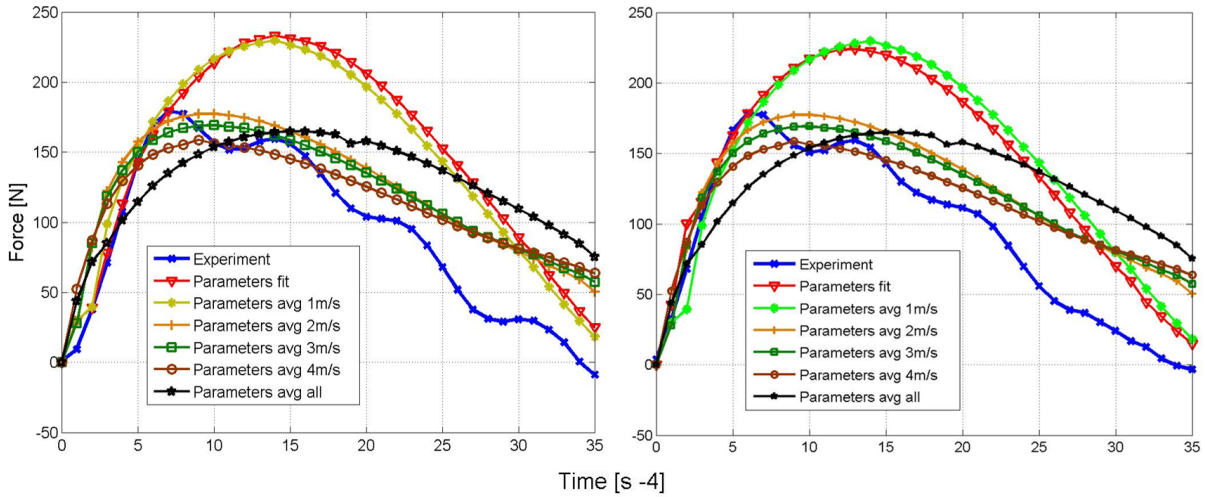

Figure 4.42: Comparison of experimental D30 behavior and FE model, impact test, impact velocity 1 m/s.

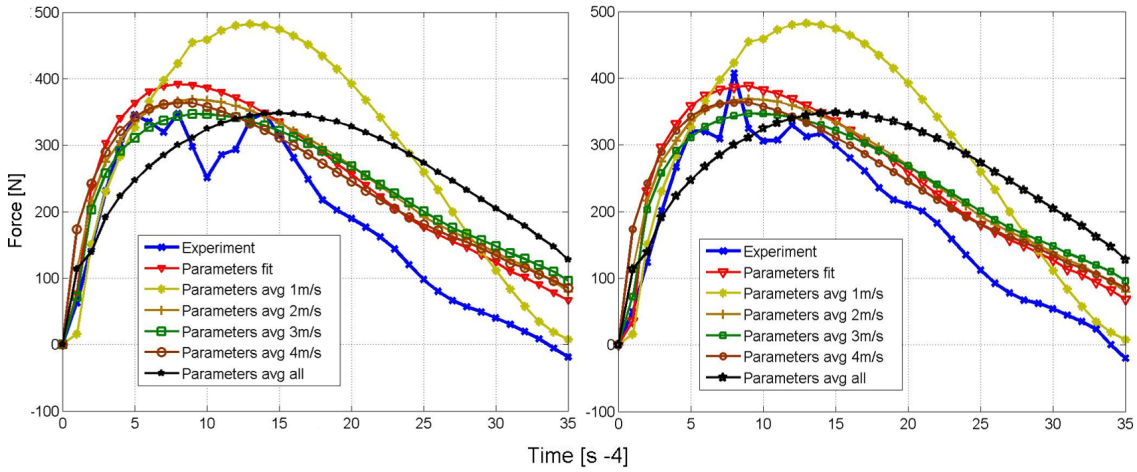

Figure 4.43: Comparison of experimental D30 behavior and FE model, impact test, impact velocity 2 m/s.

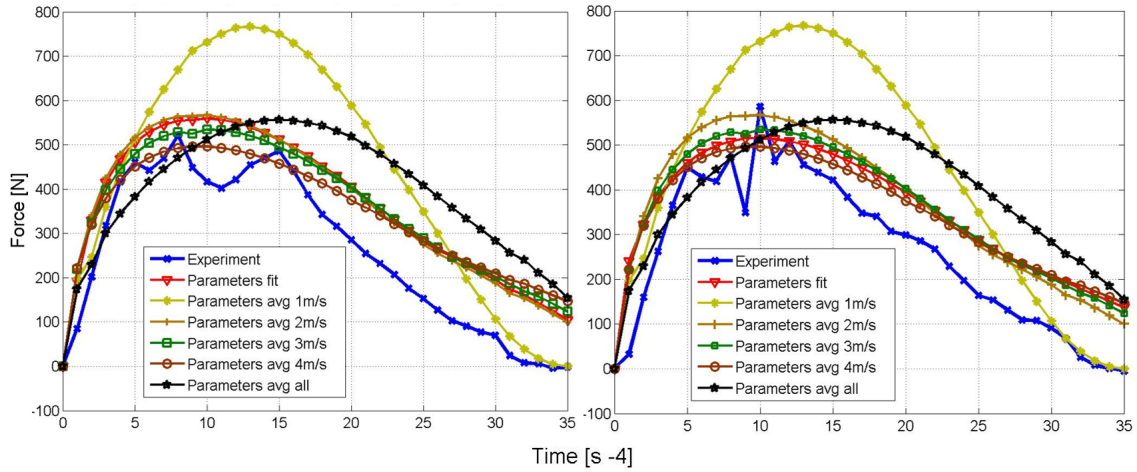

Figure 4.44: Comparison of experimental D30 behavior and FE model, impact test, impact velocity 3 m/s.

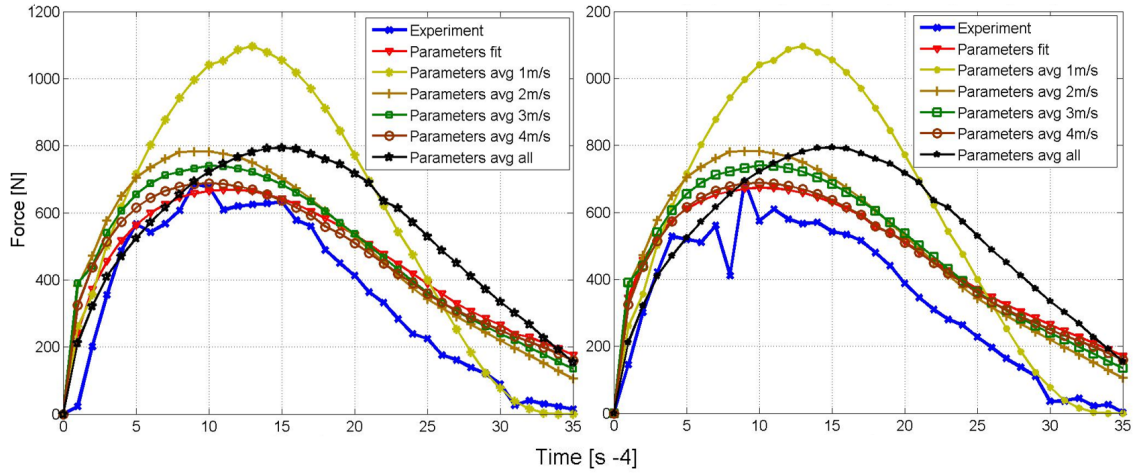

Figure 4.45: Comparison of experimental D30 behavior and FE model, impact test, impact velocity 4 m/s.

Table of the identified parameters for all the samples and impact velocities and energies was created (Tab. 4.8). The values are averaged for two tests of the same velocity. Dependencies of the particular parameters were approximated (see Figs. 4.46, 4.47 and 4.48).

Impact velocity [m/s]	Impact energy [J]	ν^{d3o}	E^{d3o} [MPa]	g_1	τ_1 [s]	g_2	τ_2 [s]	g_3	τ_3 [s]
1	0,18	0,38	1,99	0,67	10,3 e-5	0,231	24,2 e-5	0,046472	169,3 e-5
2	0,70	0,38	0,69	0,54	4,81 e-5	0,427	11,3 e-5	0,023159	79,1 e-5
3	1.58	0,38	0,62	0,56	4,31 e-5	0,415	10,1 e-5	0,022914	70,8 e-5
4	2,80	0,38	0,55	0,65	1,09 e-5	0,304	2,48 e-5	0,042572	20,4 e-5
Averaged	-	0,38	0,96	0,605	5,13 e-5	0,344	12,02 e-5	0,033779	84,9 e-5

Table 4.8: Summation of identified viscoelastic parameters.

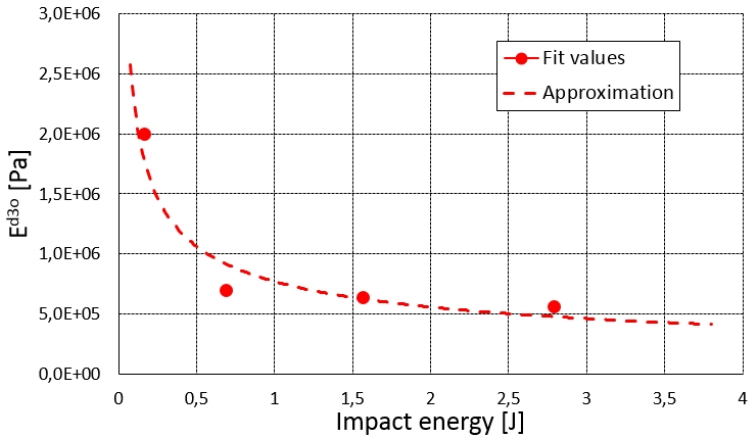

Figure 4.46: Identified values of Young's modulus of D3O for various impact energies.

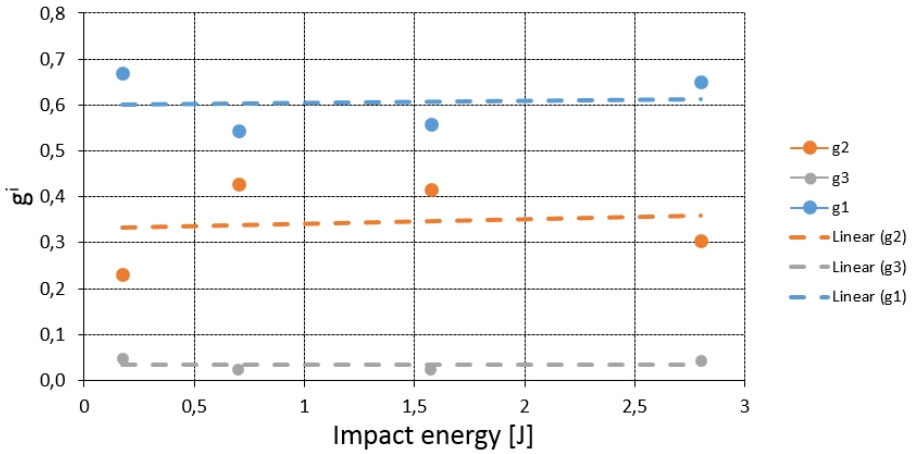

Figure 4.47: Identified values of relaxation ratio of D3O for various impact energies.

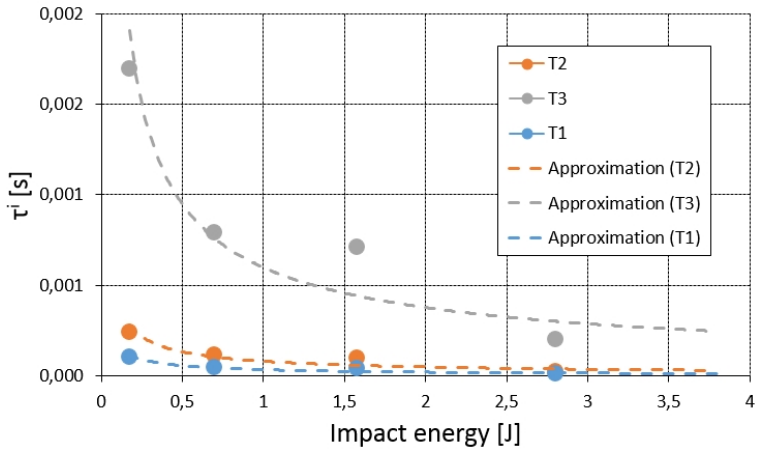

Figure 4.48: Identified stress values of relaxation time of D3O for various impact energies.

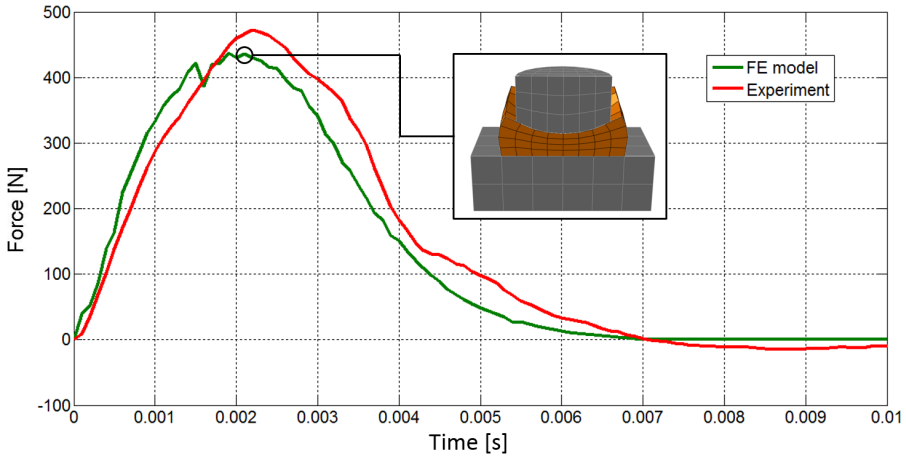

Figure 4.49: Comparison of experimental D30 behavior and FE model, impact test, semispherical impactor, impact velocity 4.5 m/s.

Parameters obtained this way were used in the model of the impact test with the semispherical impactor. The comparison of the experimental force values and the model can be seen on Fig. 4.49 and the visual comparison on Fig. 4.50.

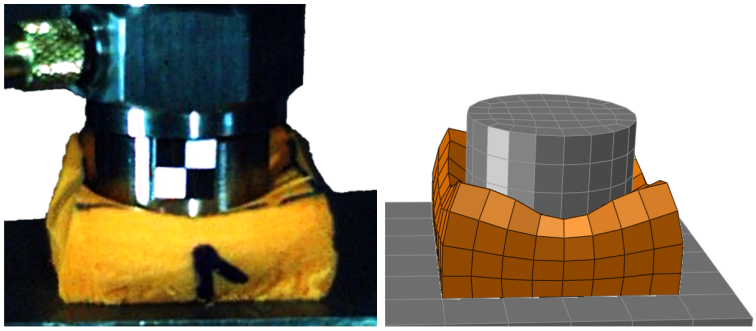

Figure 4.50: Visual comparison of experimental D30 behavior and FE model, impact test, semispherical impactor, impact velocity 4.5 m/s.

EPS elasto-plastic nonlinear model Data from the compression and impact tests were used for the identification of the elastic and plastic parameters E^{eps}, $S1$, $S2$, $S3$, $S4$, k by the identification algorithm described at Fig. 4.38.

Compression EPS compression tests were modeled the same way as D3O with the difference in the material model and displacement values (according to Tab. 4.4). Elasto-plastic model is not time dependent. Therefore, it is not capable of description of the viscoelastic relaxation behavior. The comparation of the model and the experiment can be seen on Figs. 4.51 and 4.52 where the absence of the viscoelastic behavior prevents more the accurate agreement. However, parameters obtained from the identification using this experiment were important when used as the starting values for the identification using the impact tests.

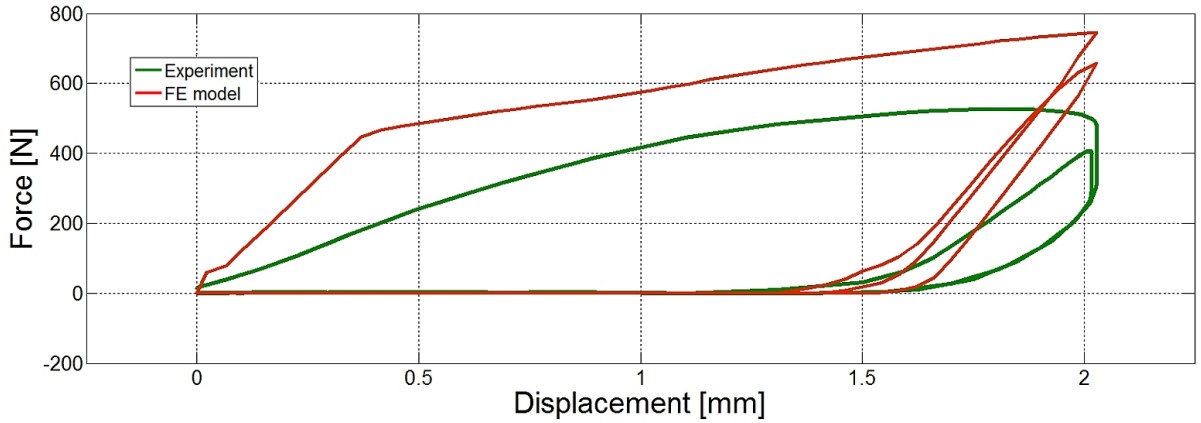

Figure 4.51: Comparison of experimental EPS behavior (sample 2) and FE model.

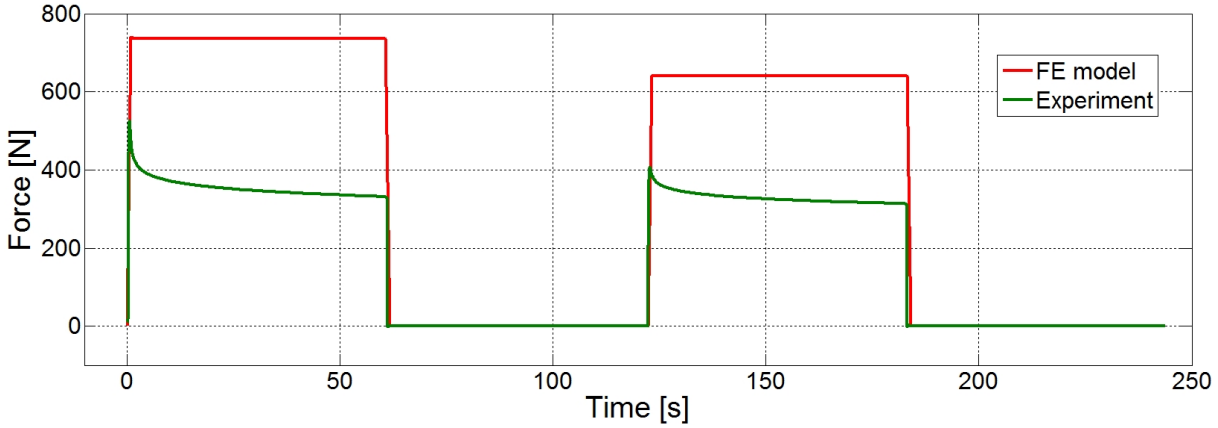

Figure 4.52: Comparison of experimental EPS behavior (sample 2) and FE model.

Impact Since EPS behavior is also strain-rate dependent, Young's modulus E^{eps} and stress values $S1$-$S4$ belonging to the plastic strain values of 0, 0.04, 0.08 and 0.11 had to be identified as well for each impact test.

The only difference among D3O and EPS impact parameters identification was that residuum was calculated only in the time points of the maximal force values. The reason was that optimization with the objective function in the form of (4.39) did not converge to the reasonable results. Figs. 4.53 and 4.54 show the aproximated dependecy of Young's modulus E^{eps} and stresses $S1 - S4$ (needed for plastic hardening curve) on the impact energy. Values of k did not show any trend, therefore, they were taken as averaged.

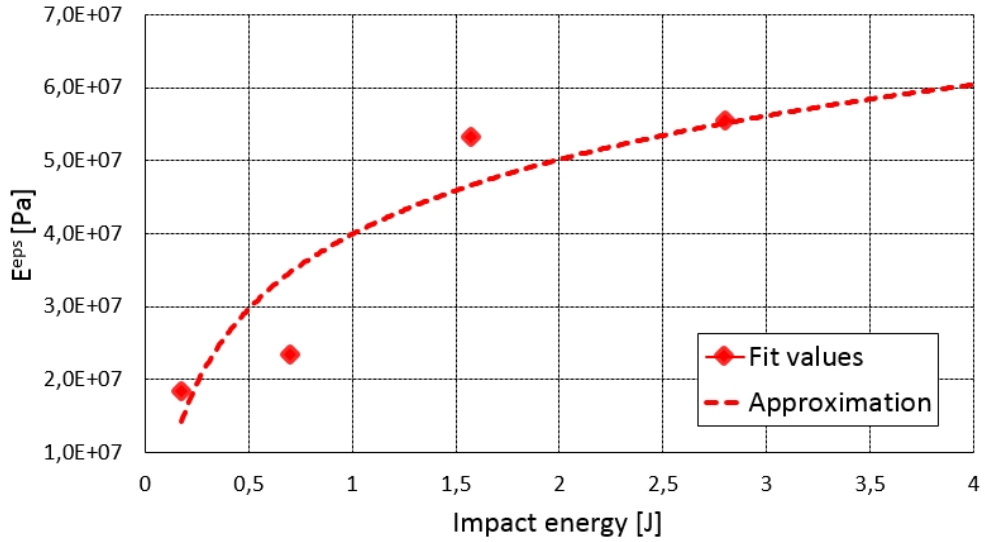

Figure 4.53: Identified values of Young's modulus of EPS for various impact energies.

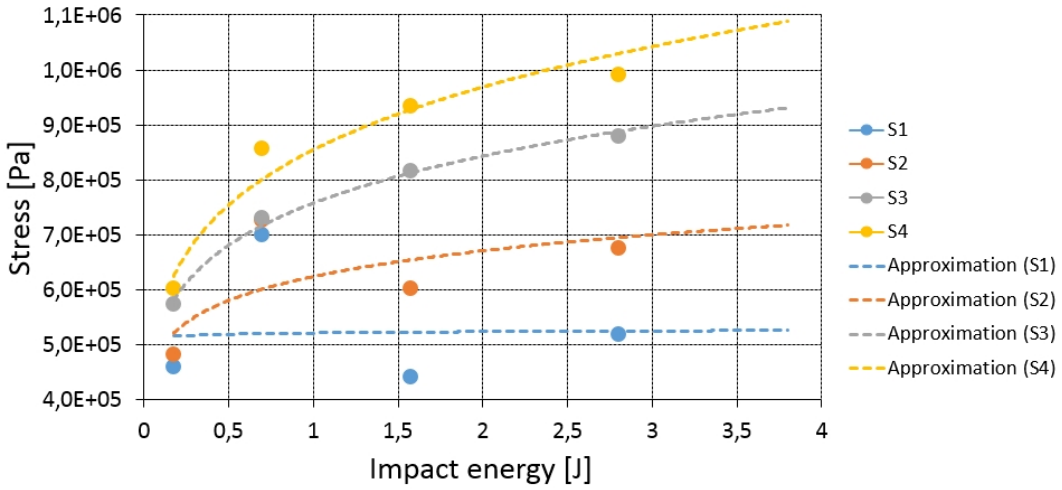

Figure 4.54: Identified stress values of plastic hardening curve of EPS for various impact energies.

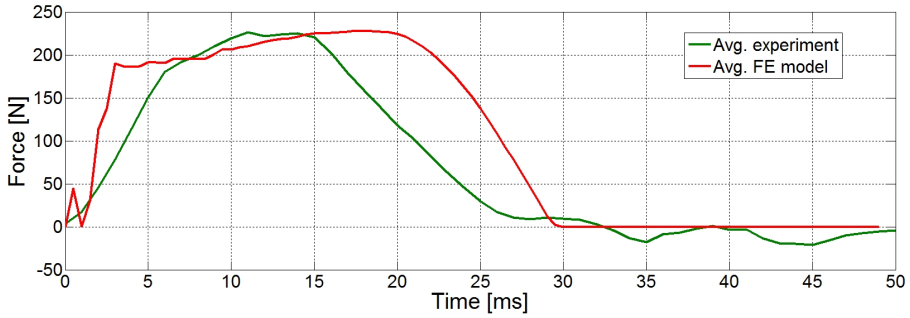

Figure 4.55: Comparison of experimental EPS behavior and FE model, impact test, impact velocity 1 m/s.

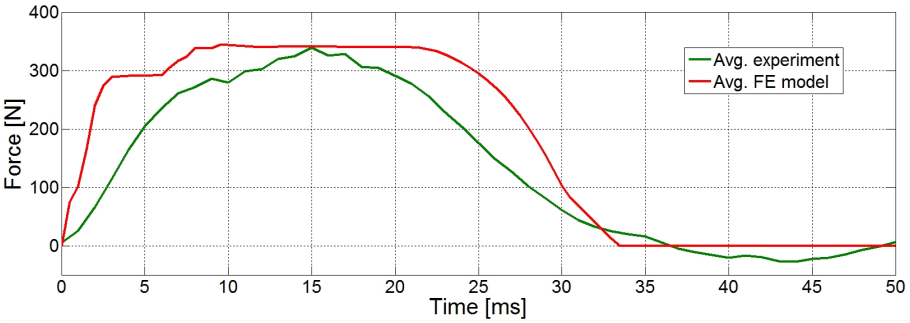

Figure 4.56: Comparison of experimental EPS behavior and FE model, impact test, impact velocity 2 m/s.

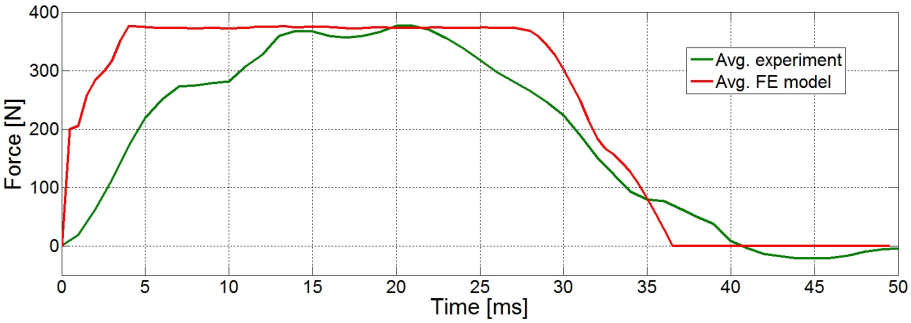

Figure 4.57: Comparison of experimental EPS behavior and FE model, impact test, impact velocity 3 m/s.

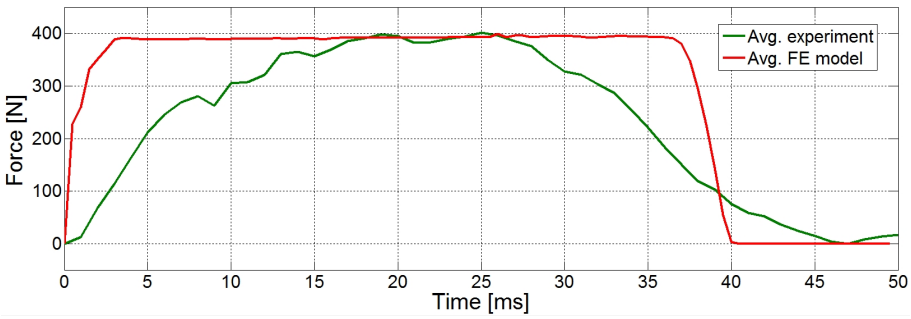

Figure 4.58: Comparison of experimental EPS behavior and FE model, impact test, impact velocity 4 m/s.

The values of the identified parameters in Tab. 4.9 and values of the forces in the comparisons of the experiments and models on Figs. 4.55 - 4.58 are averaged for two experiments/identifications of the same impact velocity. It can be observed that maximal forces of FE model and experiment are in agreement. However, FE model is stiffer in the beginning and in the end of the impact.

Impact velocity [m/s]	Impact energy [J]	ν^{eps}	E^{eps} [MPa]	$S1$ [MPa]	$S2$ [MPa]	$S3$ [MPa]	$S4$ [MPa]	k
1	0,18	0,38	18,4	0,460	0,481	0,573	0,602	1,29601
2	0,70	0,38	23,4	0,700	0,725	0,730	0,856	1,22574
3	1,58	0,38	53,2	0,441	0,602	0,815	0,935	1,07677
4	2,80	0,38	55,6	0,517	0,675	0,878	0,990	0,97711
Averaged	-	0.38	37,7	0,530	0,621	0,749	0,846	1,14390

Table 4.9: Summary of identified elasto-plastic parameters.

4.3 Combination of the outer shell and liners

Very important thing for the user's safety is how tne particular materials cooperate when assemblied together. As written before, the stiff carbon shell spreads the impact energy into the wider area. Despite the fact that D3O showed very usefull properties (no plastic deformation, strong strain rate behavior) the standard "crushable" liner is not replaceable at the moment. Therefore, combination of these three materials was proposed. EPS foam is placed between the thin carbon shell and D3O layer. That ensures that as high volume of EPS as possible is exposed to the loading. D3O liner also serves as the protection against the penetration and ensures comfortable head-helmet interface.

4.3.1 Experiments

Impacts of semispherical impactor (246 g) to the samples combined of carbon composite shell layer, EPS foam layer and D3O layer were carried out in order to validate the FE calculations with the combined material models. Geometry of the samples can be seen at Fig. 4.59. Tests were performed for impact velocities 2, 3, 4 and 5 m/s (energies 0.5, 1.1, 1.97 and 3.08 J).

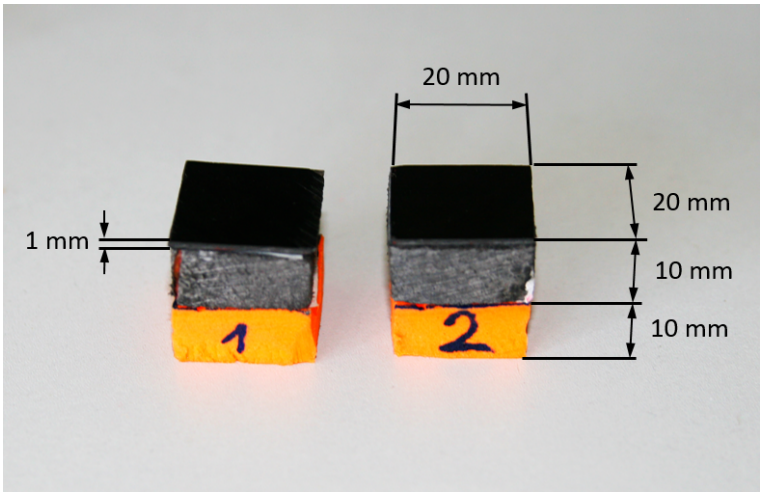

Figure 4.59: Geometry of the samples with combined materials.

4.3.2 FE models

FE model of the impact test of combined materilals is shown on Fig. 4.61 including the boundary conditions. Fig. 4.62 shows the comparison of the impact experiment and FE model. Good agreement can be observed in the beginning of the impact that also implies agreement in the acceleration. The peak of the force in FE model is lower about 15%. This disagreement could be solved by the further optimization of the combined model, nevertheless, safety coefficient is far more effective solution.

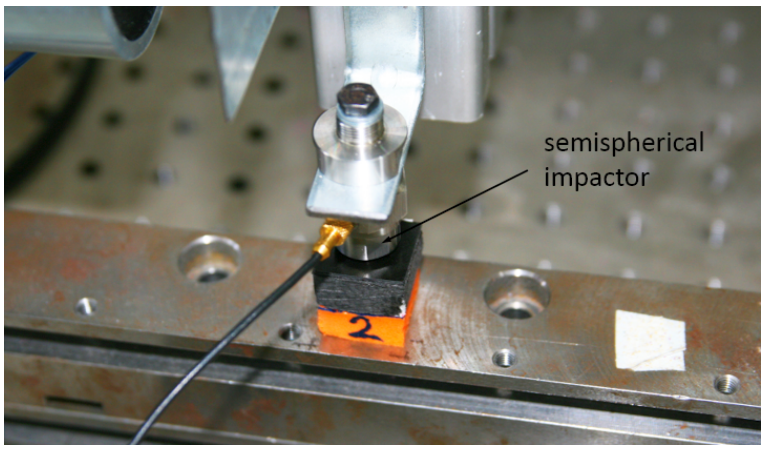

Figure 4.60: Samples with combined materials in the testing device.

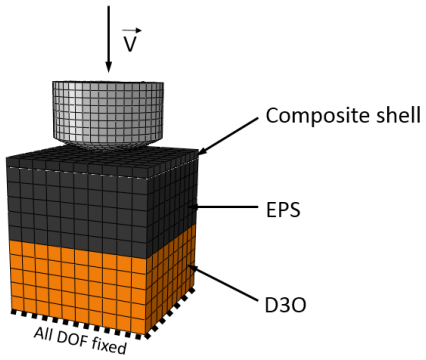

Figure 4.61: FE model of the impact test of combined materials.

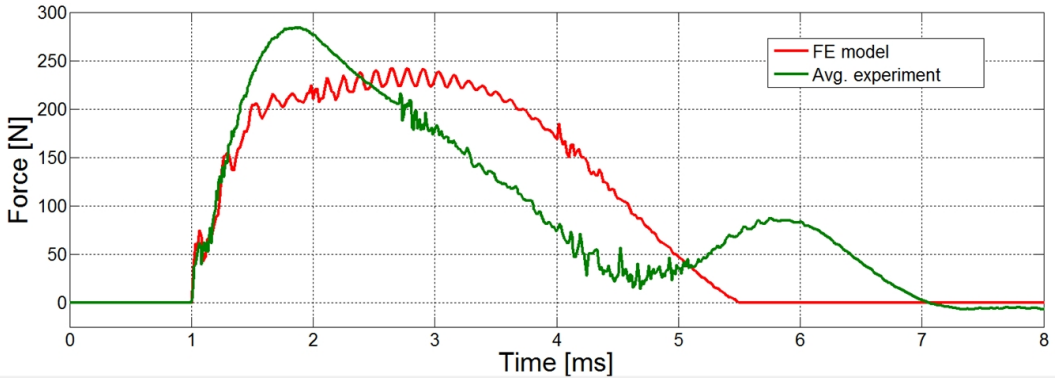

Figure 4.62: Impact test of combined materials, semispherical impactor, imapct velocity 2 m/s.

4.3.3 Summary

Althought only the impact criteria mentioned in ČSN EN standards were considered in this work, there are more biomechanical aspects that can be considered in helmet design. One of them was mentioned before - the brain rotation. The most of the real life impacts are not happening in the perpendicular direction. Therefore, based on the first newton law, shape of the skull and the other aspects, the certain amount of impact energy is transfered

into the rotation of the brain, that can cause serious concussion.

Hence, the liner able of easier tangential deformation was proposed. It consists of two "conical-shaped" layers - EPS and D3O. One cell of the conical liner can be seen on Fig. 4.63.

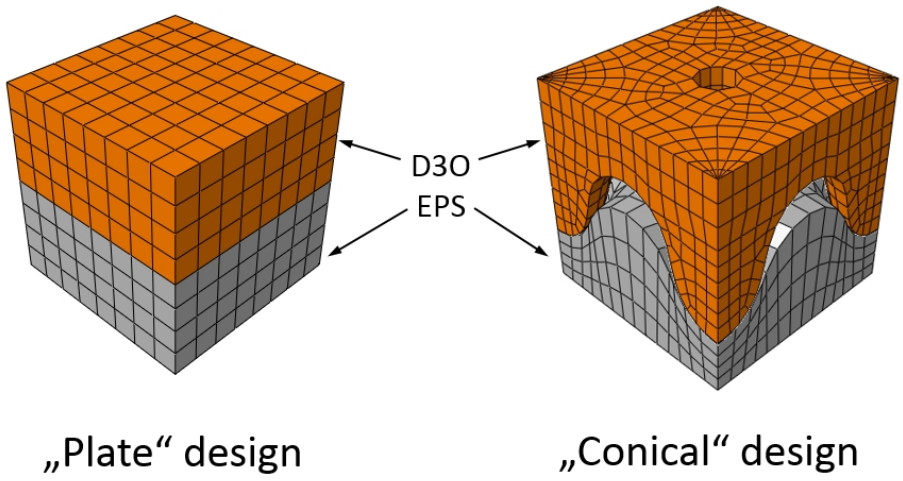

Figure 4.63: Proposed conical liner compared with the standard liner.

The sequence of layers can be the same as written above. Unfortunatelly, because of the scope of this work, this design could not be implemented into the final FE models of the helmet. However, to show that such a design would be capable of passing ČSN EN standards, the simple impact test in the perpendicular direction was modelled and the results were compared with standart "plate" liner. It can be observed on Fig. 4.64 that the reaction force in the simulated impact test increased only gently in the new design. Moreover, it brings significant 20% weight save.

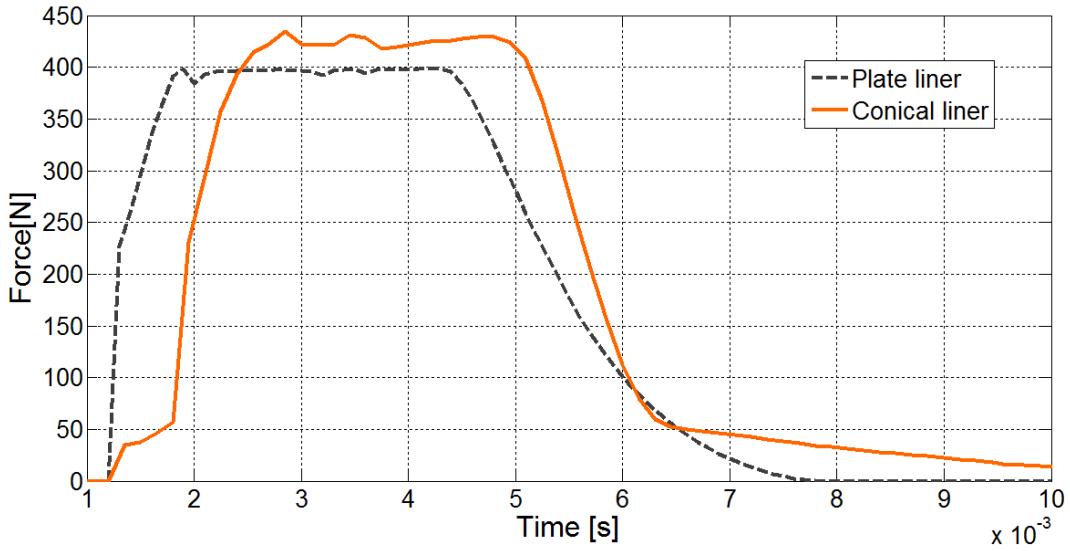

Figure 4.64: Impact test, flat 350g impactor, impact velocity 4m/s. Comparation of plate and conical liner design

Chapter 5

Final design

5.1 Sketches

A lot of versions proposed in the form of sketches were considered for the detailed study. One of the main issues was whether make the helmet changeless for all the sports (for example half-face version on Fig. 5.1) or enable more configurations depending on which sport is helmet going to be used for (version with removable chin guard and visor on Figs. 5.2 and 5.4).

It was decided that only the configureable version can fullfill requirements emerging from Selection of properties. The final design consist of these features:

- Upper part of the helmet without any ventilation holes protecting the user from the falling objects (requirement of mounitain helmet)
- Long plastic peak adjustable by two ergonomic nuts.
- Removable visor anchored to the peak.
- Triangular lateral holes enabling enough ventilation whereas keeping the simple rib construction.
- Two main ventilation holes in the front and in teh rear part of the helmet highlighted by integrated led-stripes.
- Extented rear part protecting user's nape and enabling connection of the chin guard.
- Removeable ching guard for tougher activities (enduro biking, downhill biking and skiing, paragliding...)
- Mutipurpose tray on the top of the helmet enabling connection of various accessories (camera mounts, battery cells, torch mounts...)

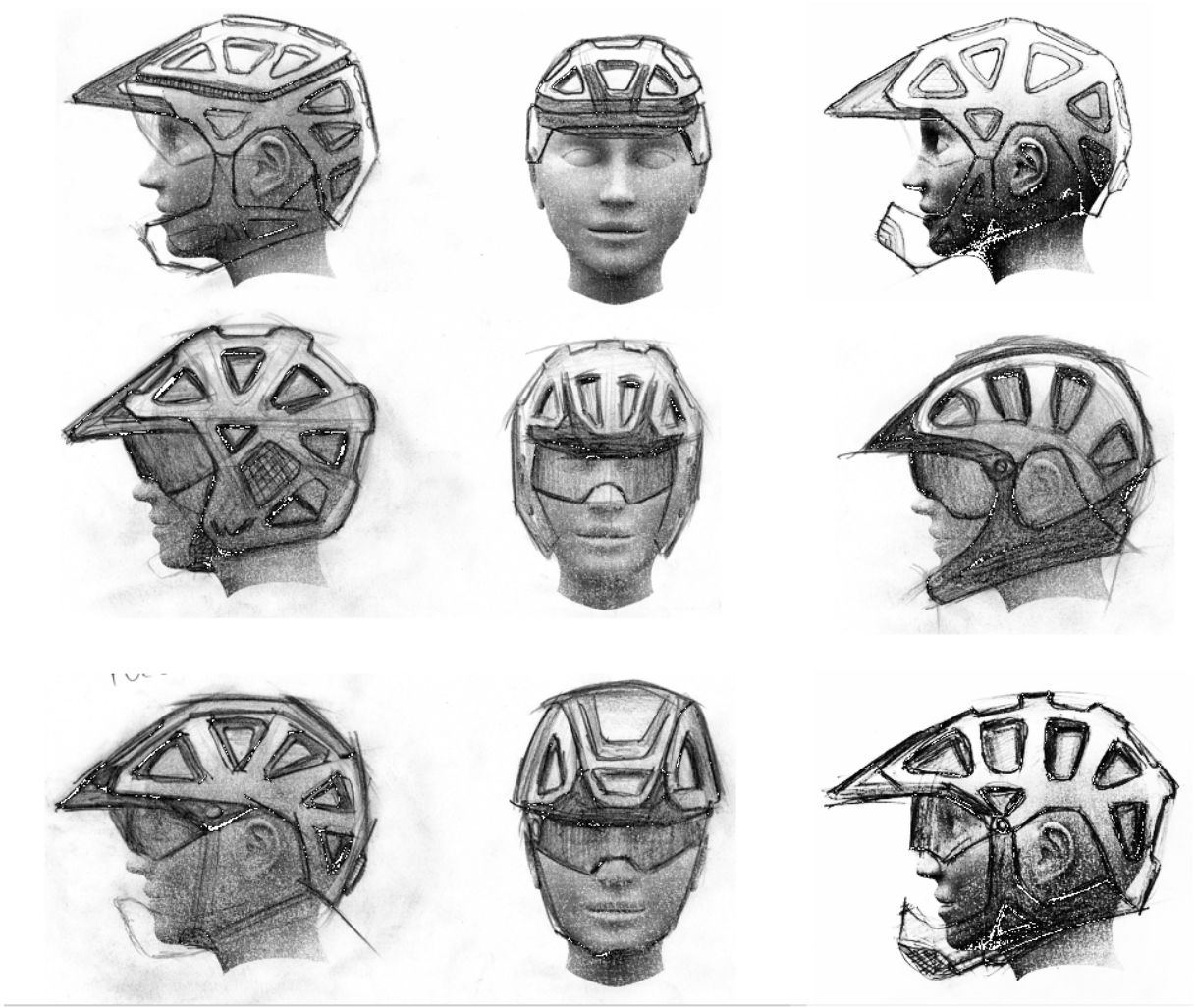

Figure 5.1: Sketches.

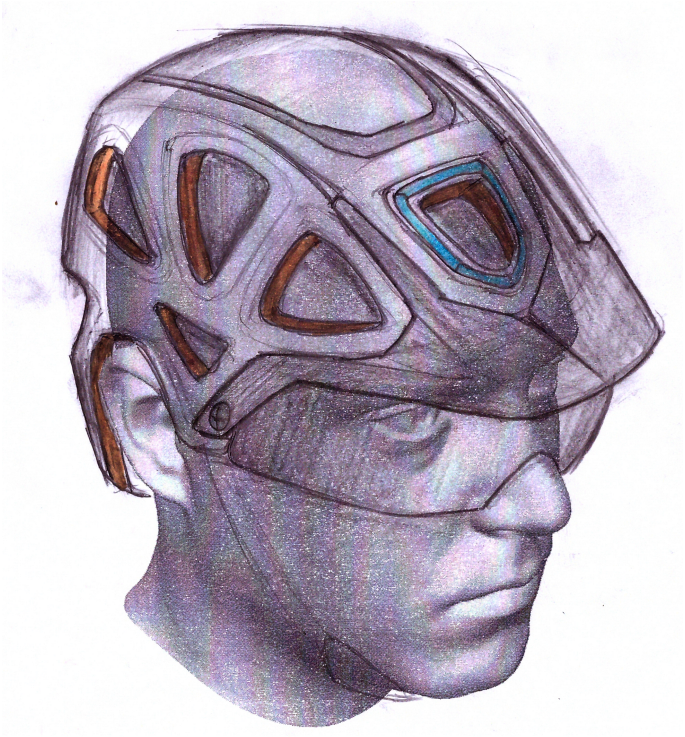

Figure 5.2: Sketch of the final version - light configuration for cycling, in-line, equestrian sports or mountaineering.

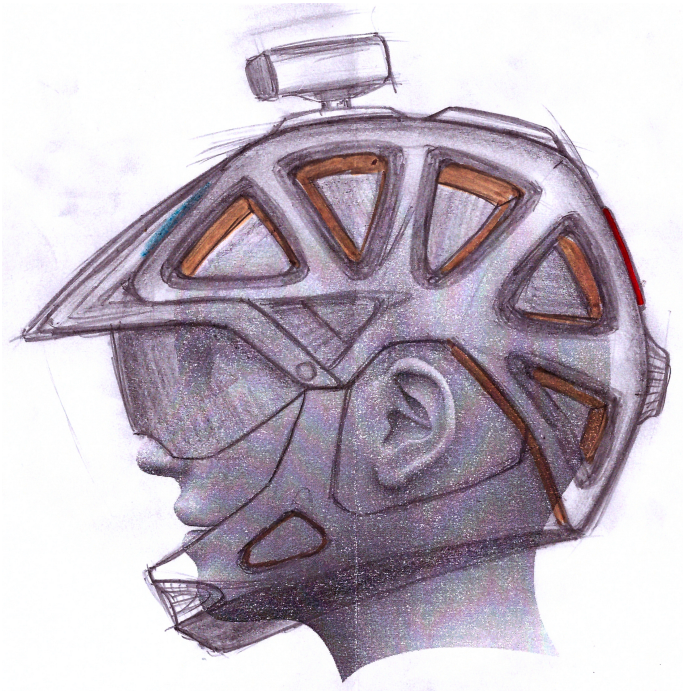

Figure 5.3: Sketch of the final version - full configuration for enduro cycling, downhill skiing or paragliding.

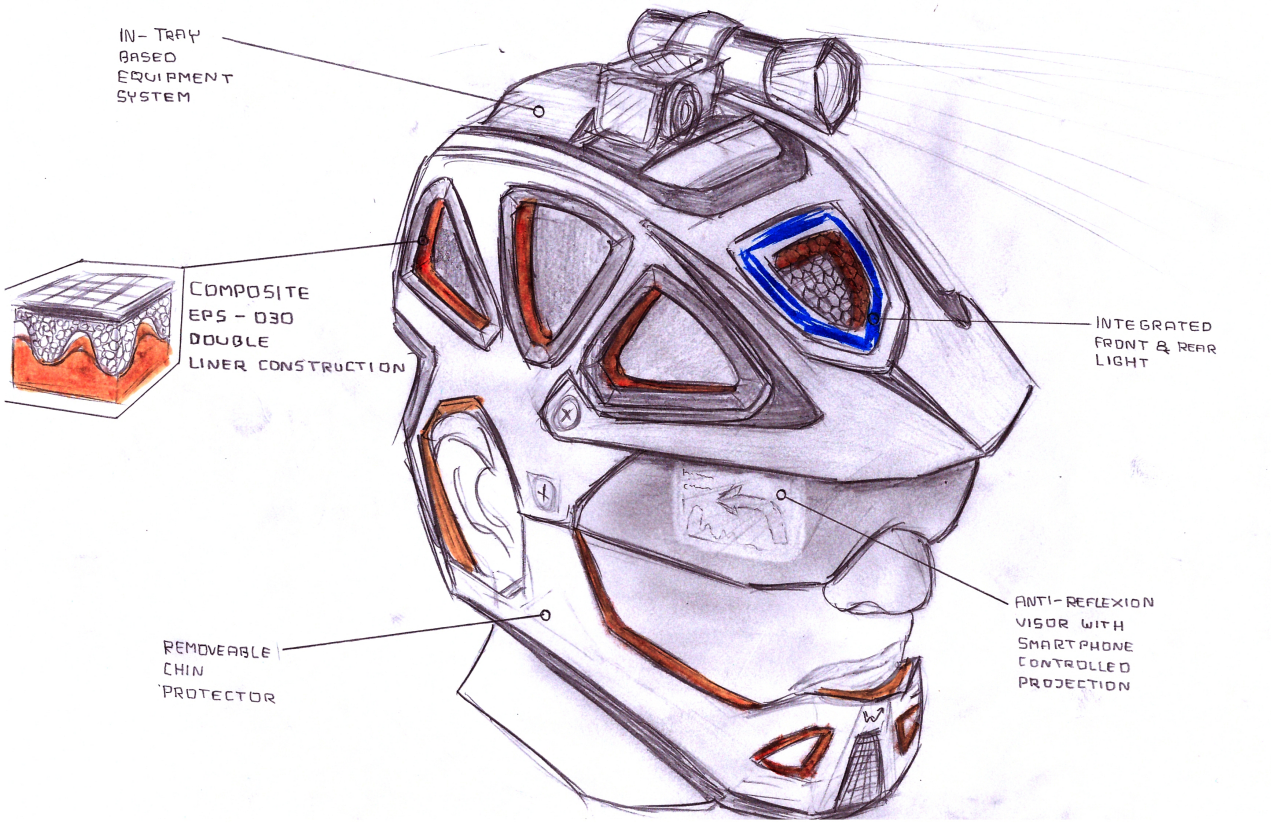

Figure 5.4: Sketch of the final version - full configuration for enduro cycling, downhill skiing or paragliding.

5.2 FE calculation

Material models ivestigated in the previous chapter were used to create the FE models of the whole standartized ČSN EN impact tests. Headform with the circuit of 555 mm was modeled using spherical coordinates given in EN 960 standard. Geometry of the impact anvils was given by the parcitular standards. Fig. 5.9 shows the whole assembly of the outer shell, liners and headform. Composite outer shell was modeled by linear shell elements, liners and headform by hexagonal linear elements.

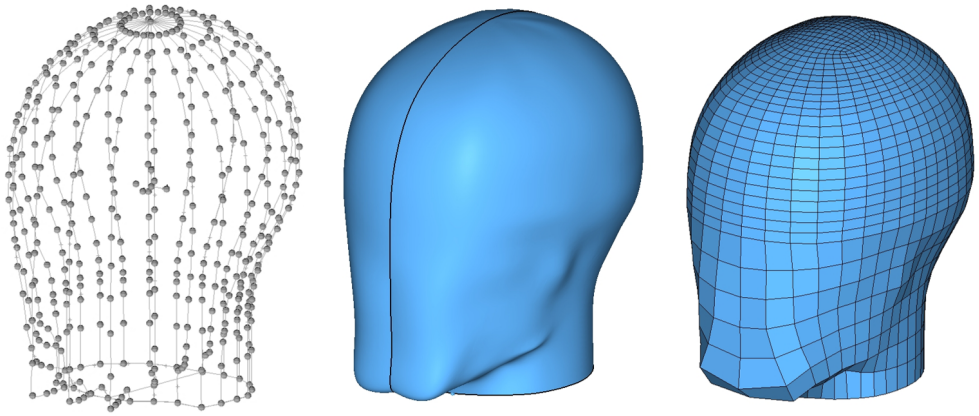

Figure 5.5: Headform of circumference of 555 mm according to EN 960 standard. Given coordinates on the left, approximated geometry in the center and FE mesh on the right.

The process of estimation of the material parameters for the particular models is described on Figs. 5.6 and 5.7. Description of the fibre architecture and laminate thickness in the outer shell can be observed on Fig. 5.8. Laminate of 2 mm thickness consists of variable number of laminas that depends on the part of the helmet. Flat central part was designed as the unidirectional core (the fibres are oriented in the front-rear direction) covered symmetrically by two laminas of the orientation of the fibres +- 45° (where the reference direction 0° is represented by direction of the core). In the case of the lateral, frontal and rear ribs, the laminate was designed the same way with the only exception that the unidirectional core is oriented by the direction of the ribs. Then there are spots, where the fibres of particular ribs cross each other. At that spots, laminate contains bi-axial core (two unidirectional cores joined together) and the symmetrical cover of the orientation of +-45° again. The edges of the ventilation holes were designed as wrapped by one unidirectional layer. This whole approach of interconnected continuos laminas should prevent the construction from the stress concentrators. All the holes would be already included as the negative shapes in the potentiall mould and they would be wrapped instead of cut out.

Hashin damage initiation criterion and energy based continuous damage were considered for the composite. An ideal connection between the composite shell, EPS and D3O was considerd. No peak, visor, chin strap and retaining mechanism were included in the models.

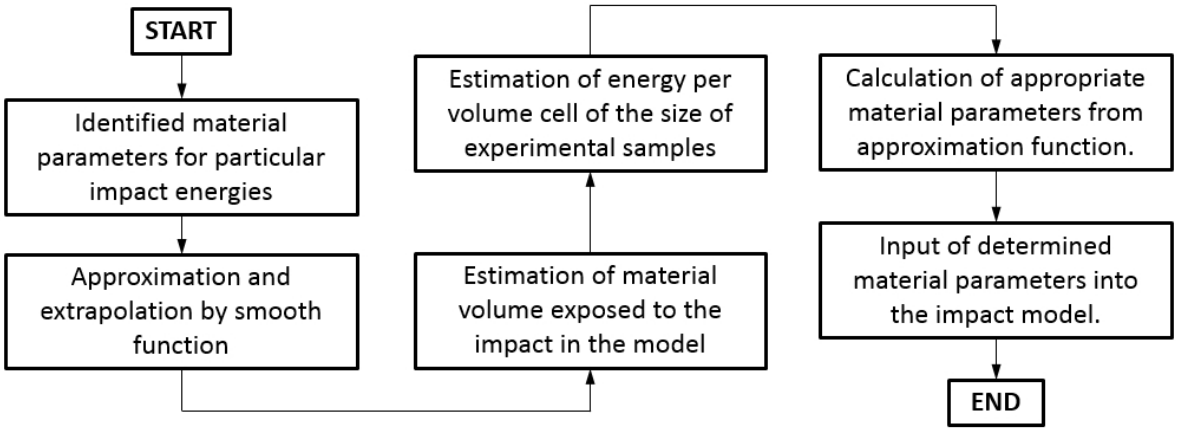

Figure 5.6: Descriprion of the determination process of the material parameters.

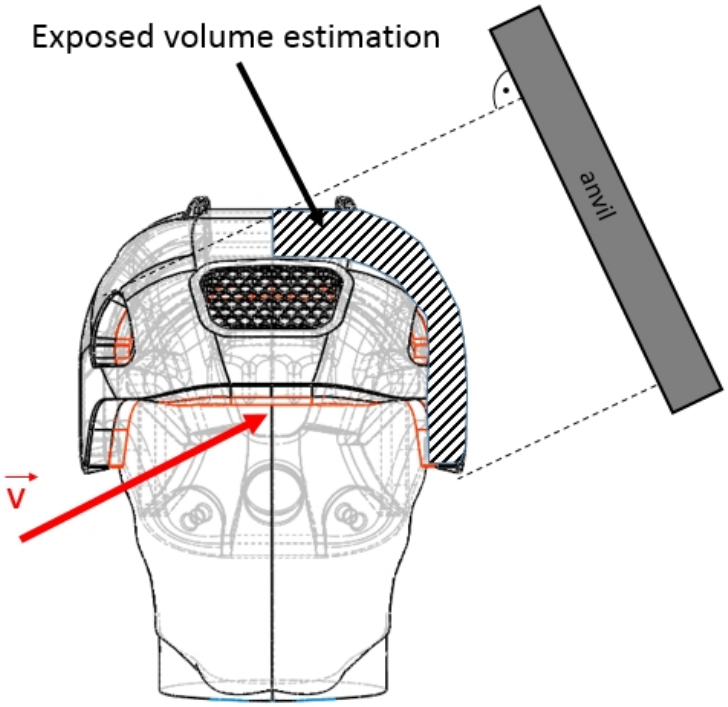

Figure 5.7: Scheme of the estimation of the exposed volume.

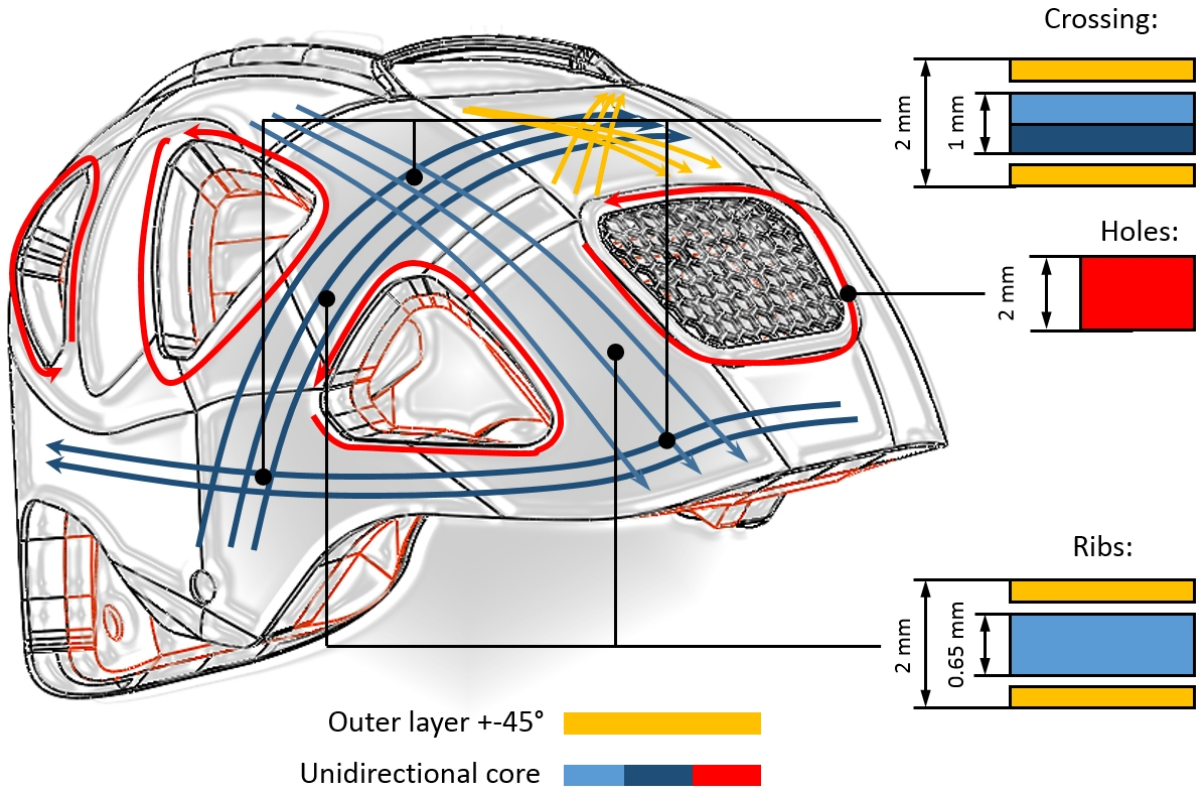

Figure 5.8: Scheme of the fibre architecture in the carbon composite laminate shell.

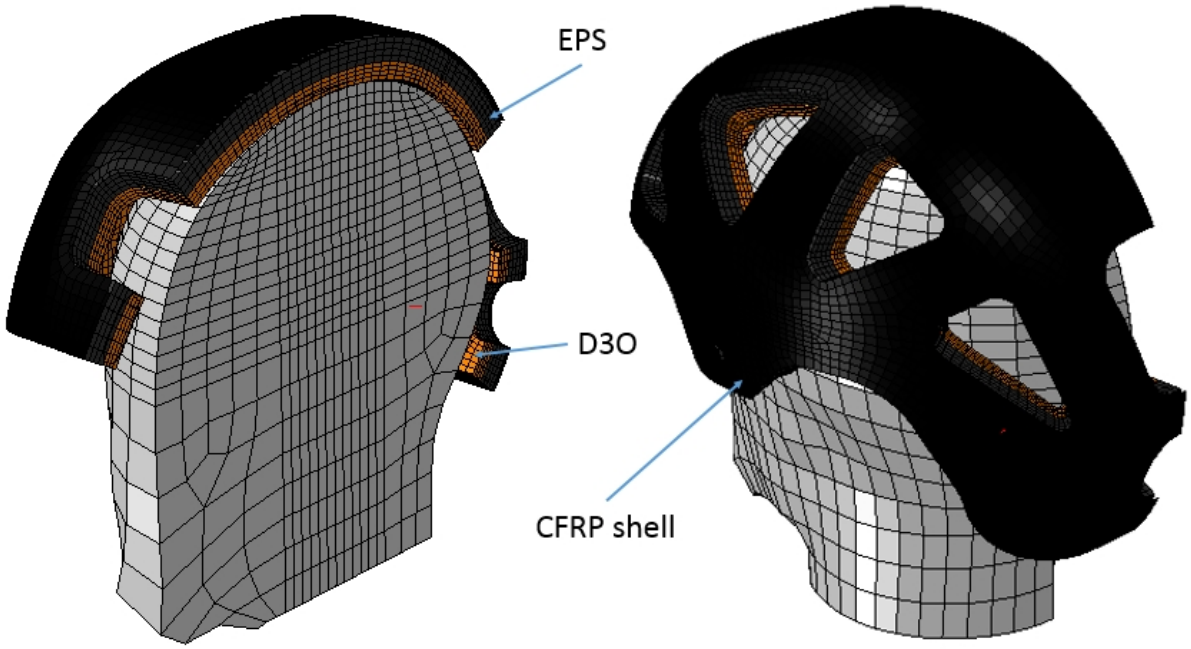

Figure 5.9: FE mesh of the final assemby - headform, D3O liner, EPS liner and outer carbon fibre composite shell.

ČSN EN 1078 - Helmets for pedal cyclists and for users of skateboards and roller skates. The whole test contains of two subtests - free fall of the helmet strapped on the headform to the flat anvil (impact velocity 5,42 m/s, Fig. 5.10) and to the kerb anvil (impact velocity 4.57 m/s, Fig. 5.13).

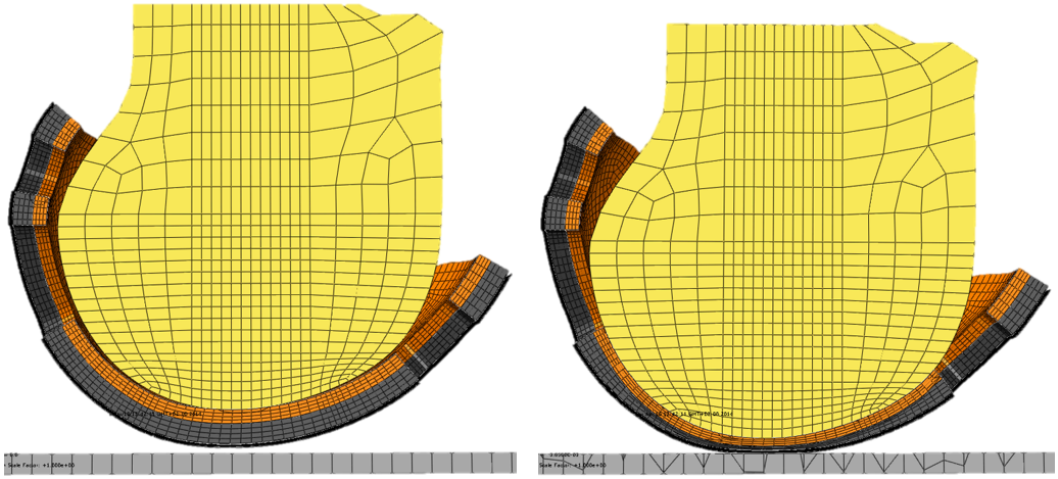

Figure 5.10: ČSN EN 1078 - Helmets for pedal cyclists and for users of skateboards and roller skates. Flat impact anvil. Impact energy 54 J. FE model.

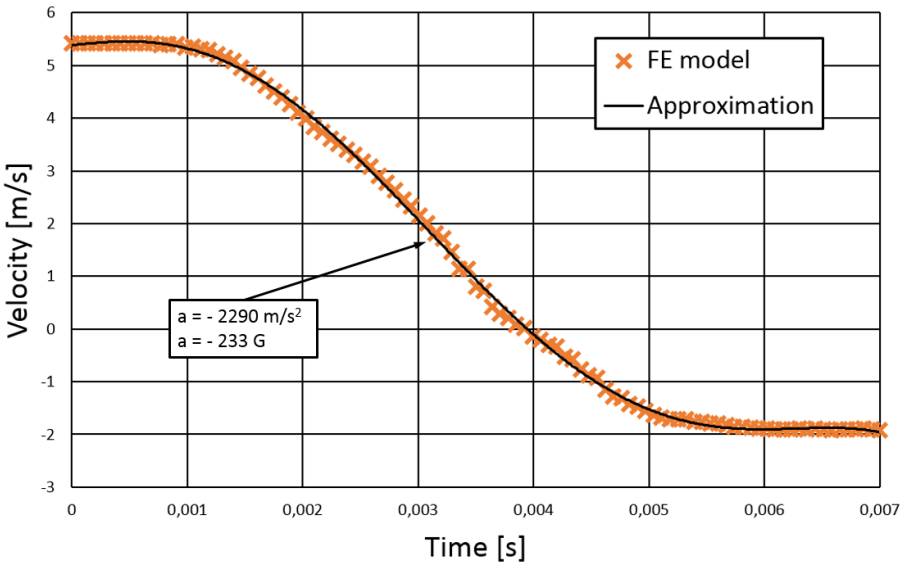

Figure 5.11: ČSN EN 1078 - Helmets for pedal cyclists and for users of skateboards and roller skates. Flat impact anvil. Impact energy 54 J. Maximal decceleration 233 G.

Values of the velocity in the particular time points were polynomially approximated in order to get the differentiable function. Value of the maximal decceleration were then obtained by differentiation of this polynomial velocity approximation (Figs. 5.11, 5.13, 5.23).

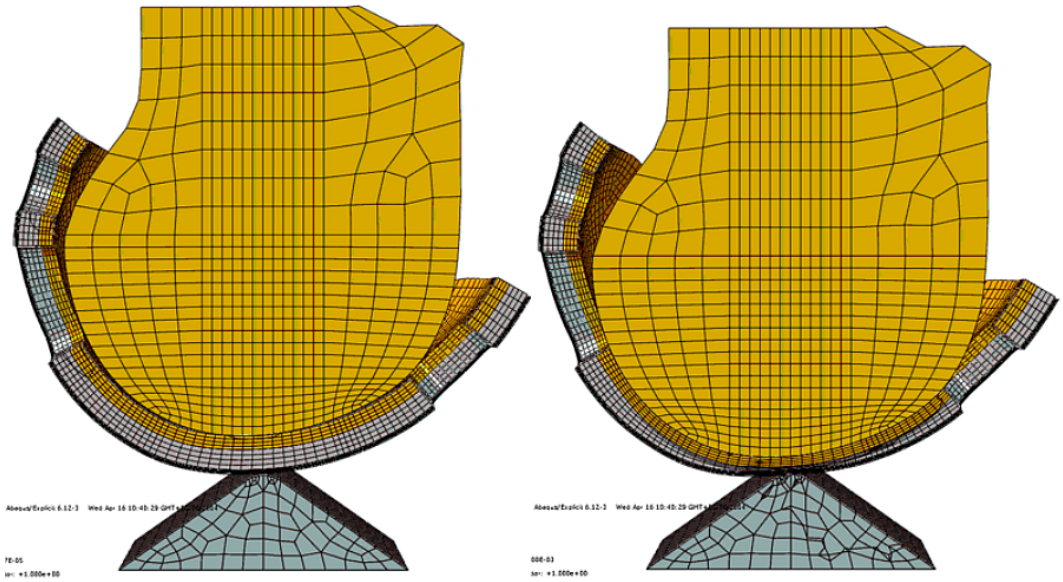

Figure 5.12: FE model of ČSN EN 1078 - Helmets for pedal cyclists and for users of skateboards and roller skaters. Kerb impact anvil. Impact energy 34 J. Maximal decceleration 192 G.

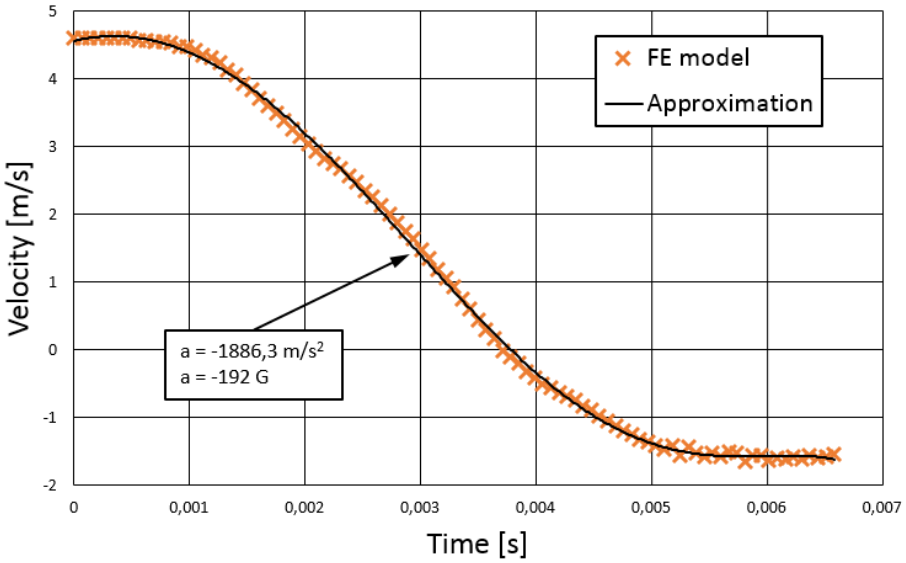

Figure 5.13: ČSN EN 1078 - Helmets for pedal cyclists and for users of skateboards and roller skaters. Kerb impact anvil. Impact energy 34 J. Maximal decceleration 192 G.

ČSN EN 12 492 - Helmets for mountaineers. The whole test contains of four subtests - free fall of the hemispherical weight (5 kg) from 2 metres to the helmet strapped on the fixed headform (Fig. 5.20), and free falls of the flat anvil (5 kg) from 0.5 meter to the front (Fig. 5.14), lateral (Fig. 5.16) and rear (Fig. 5.18) part of the helmet under the angle of 30° (measured from the main headform plane).

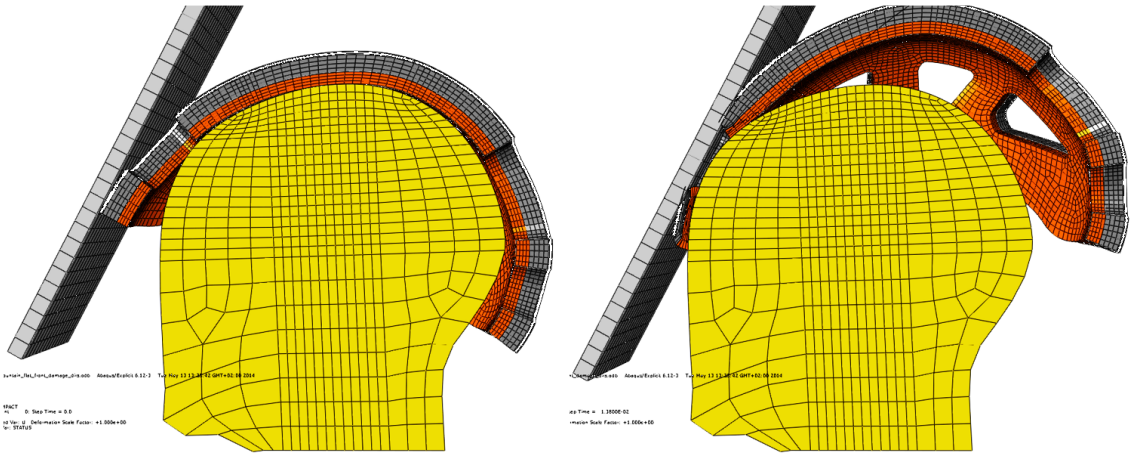

Figure 5.14: ČSN EN 12 492 - Helmets for mountaineers. Front impact. Impact energy 24.5 J. Maximal transferred force 3193 N.

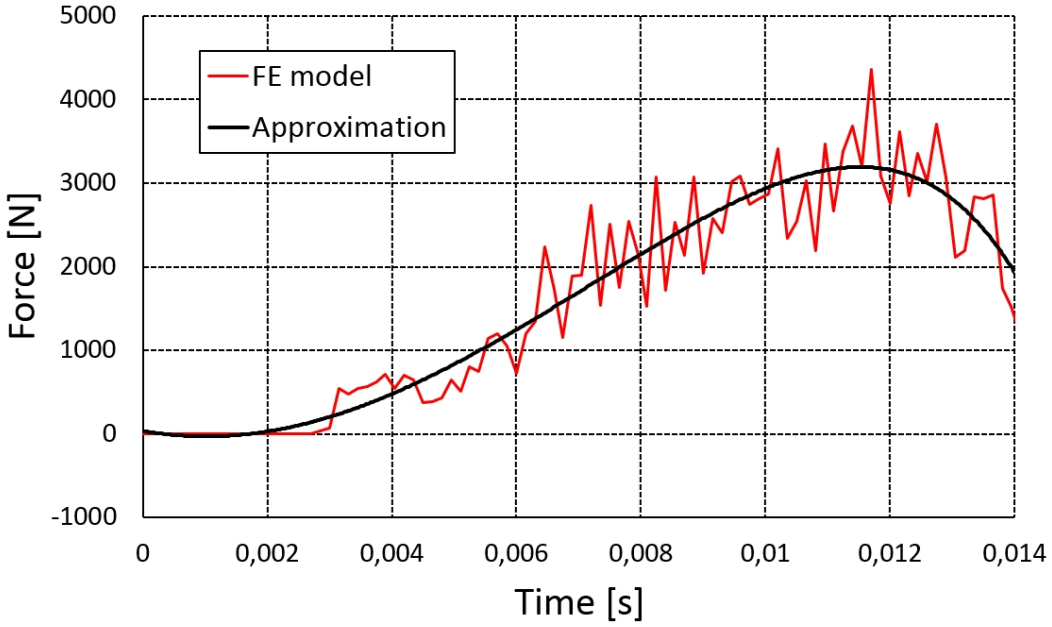

Figure 5.15: ČSN EN 12 492 - Helmets for mountaineers. Front impact. Impact energy 24.5 J. Maximal transferred force 3193 N.

Because the frequency of the physicall force sensor used in the real experiments is not known and the value of the maximum force strongly depends on this frequency, values from the model were approximated by polynomial functions and the maximum forces were considered as the peaks of these functions (Figs. 5.15, 5.17, 5.15 and 5.21).

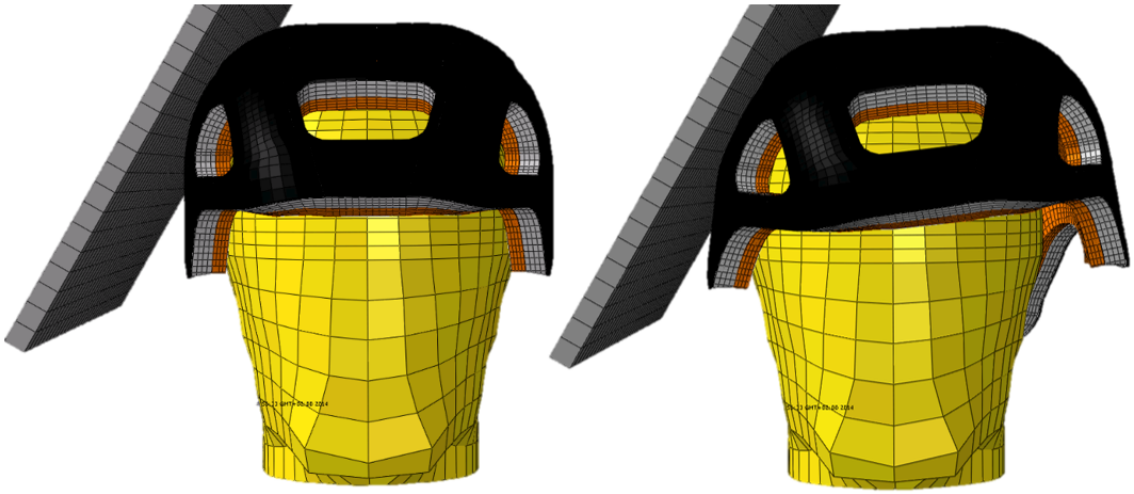

Figure 5.16: ČSN EN 12 492 - Helmets for mountaineers. Side impact. Impact energy 24.5 J. Maximal transferred force 5000 N.

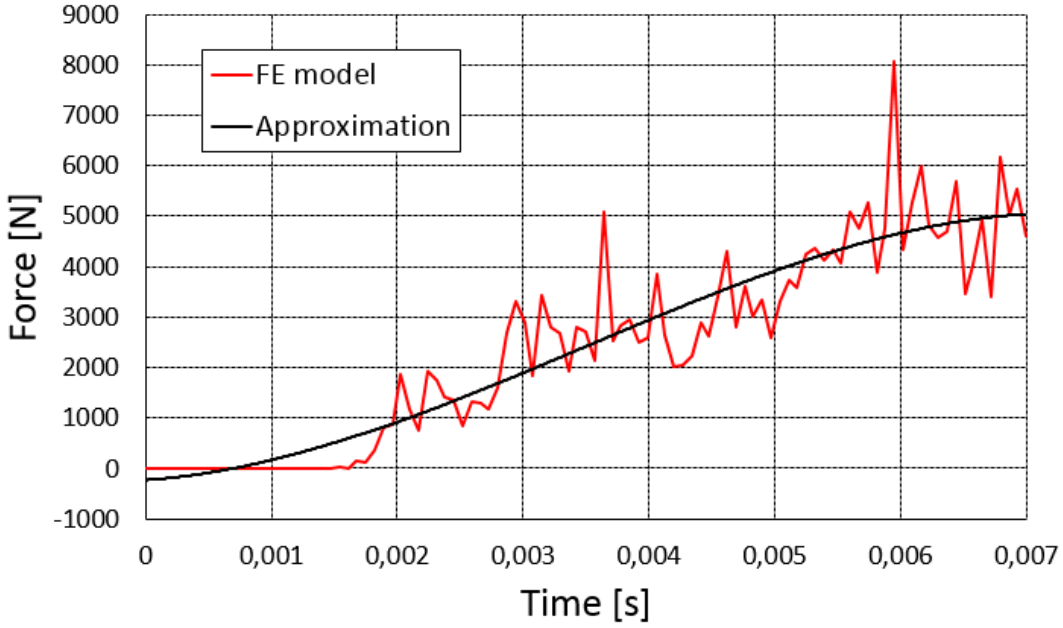

Figure 5.17: ČSN EN 12 492 - Helmets for mountaineers. Side impact. Impact energy 24.5 J. Maximal force 5000 N.

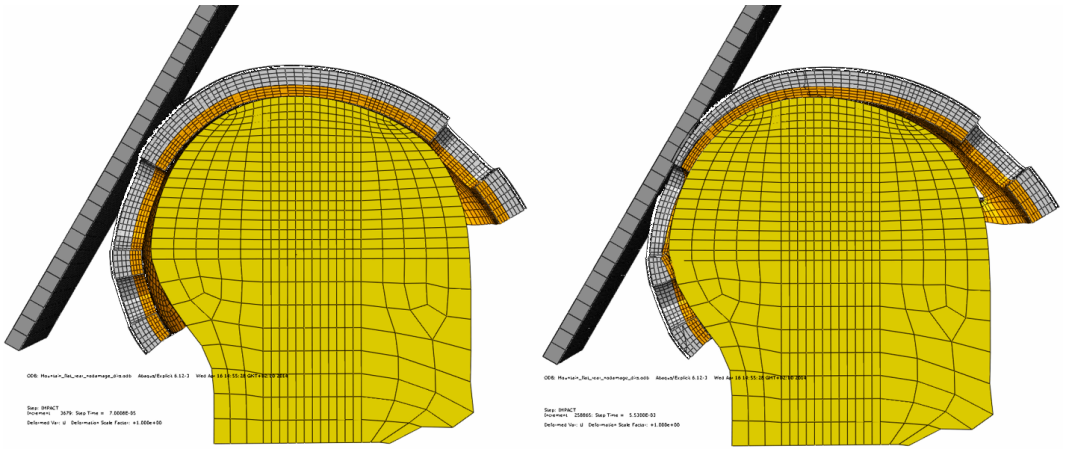

Figure 5.18: ČSN EN 12 492 - Helmets for mountaineers. Rear impact. Impact energy 24.5 J. Maximal transferred force 5353 N.

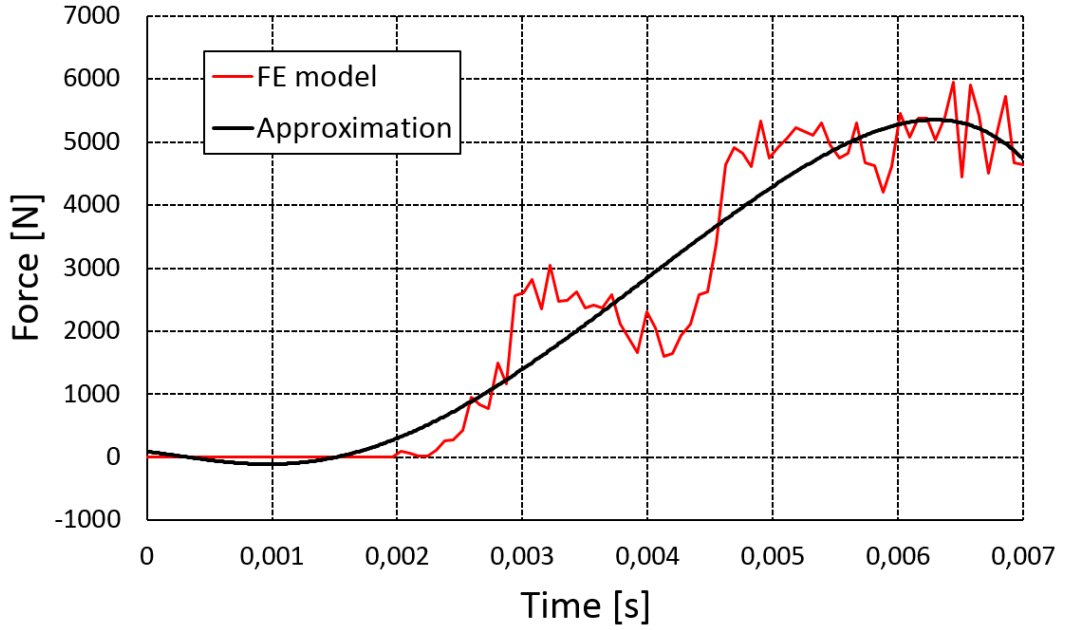

Figure 5.19: ČSN EN 12 492 - Helmets for mountaineers. Rear impact. Impact energy 24.5 J. Maximal transferred force 5353 N.

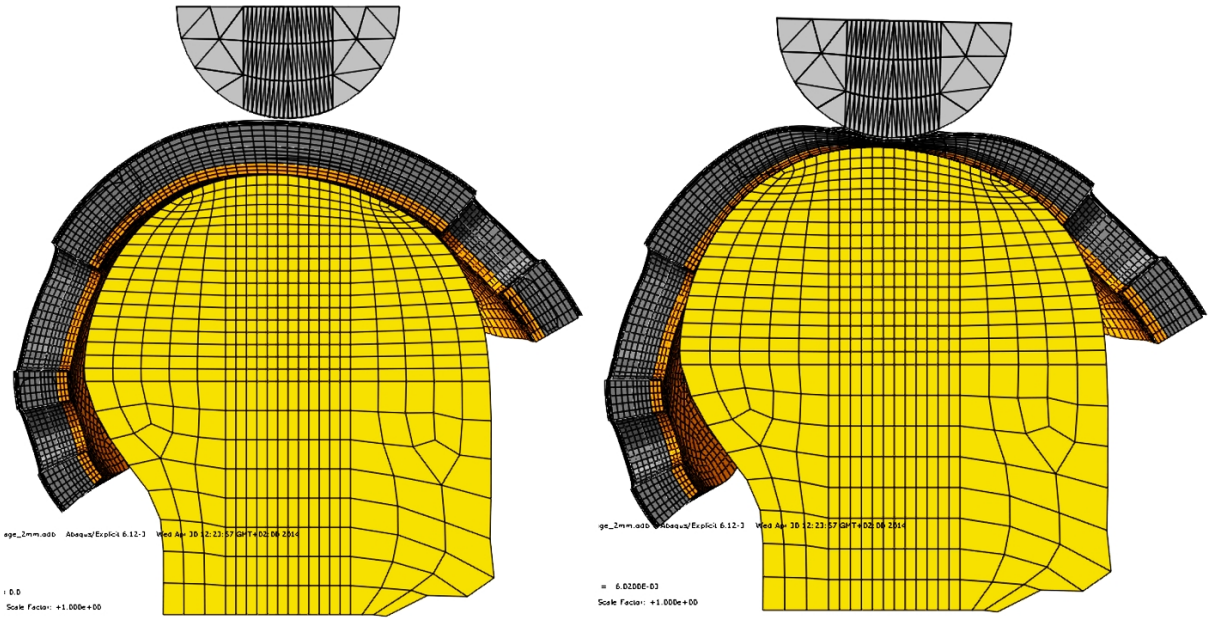

Figure 5.20: ČSN EN 12 492 - Helmets for mountaineers. Perpendicular impact. Impact energy 98 J. Maximal transferred force 10119 N.

It was deduced from the previous tests that original geometry with liner consisted of 10 mm EPS and 7 mm D3O would not pass the test. Therefore thickness of the liner was adjusted to 20 mm of EPS and 5 mm of D3O.

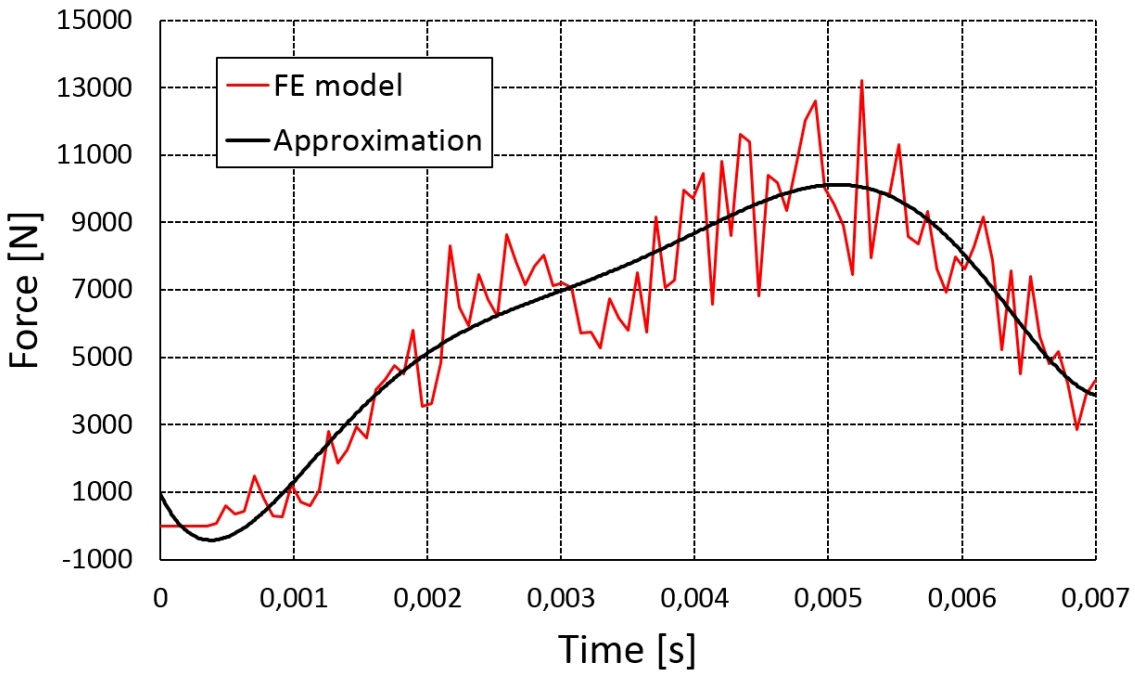

Figure 5.21: ČSN EN 12 492 - Helmets for mountaineers. Main impact. Impact energy 98 J. Maximal transferred force 10119 N.

ČSN EN 1385 - Helmets for canoying and white water sports. The test contains of free fall of the helmet (strapped to the headform) to the hemispherical anvil with impact velocity of 3,11 m/s.

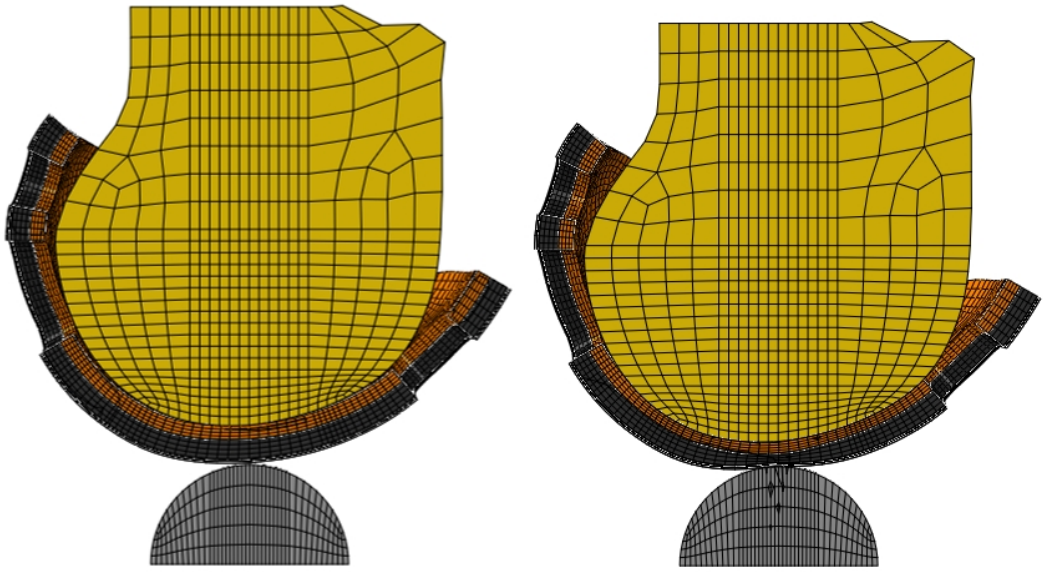

Figure 5.22: ČSN EN 1385 - Helmets for canoying and white water sports. Impact energy 35.8 J. Maximal decceleration 105 G.

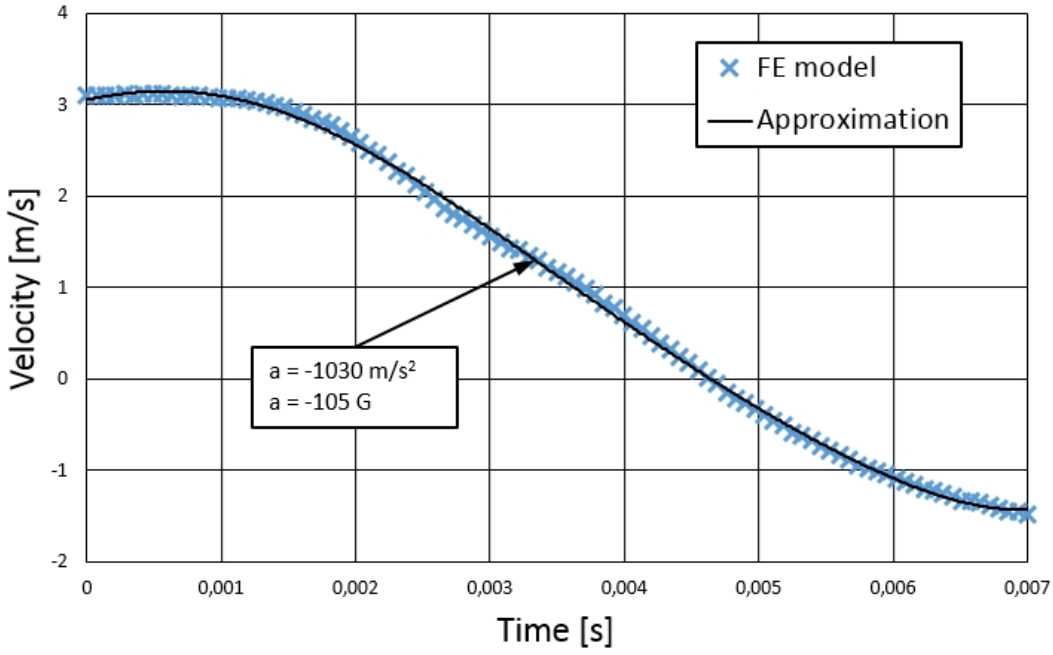

Figure 5.23: ČSN EN 1385 - Helmets for canoying and white water sports. Impact energy 35.8 J. Maximal decceleration 105 G.

ČSN EN 1384 - Helmets for equestrian activities. Conditions of the impact test are identical to the flat anvil test of ČSN EN 1078.

ČSN EN 966 - Helmets for airborne sports. Conditions of the impact test are identical to the flat anvil test of ČSN EN 1078.

ČSN EN 1077 - Helmets for alpine skiers and snowboarders. Conditions of the impact test for the ligter A helmet version are identical to the flat anvil test of ČSN EN 1078.

5.3 Summary

As can be observed from Figs. 5.10 - 5.23 the results for the final design met the safety requirements in all cases excluding the perpendicular impact in test concerning the helmets for mouintaineers. It would be possible to extend the thickness of the liner to get the higher safety. Unfortunatelly, this approach would be in conflict with condition of the low volume of the helmet for mountaineering. Thus, based on the FE results only, it would has to be claimed that final design would not be certified as the mouintaineering helmet. It also has to be kept in mind that FE model of the cell made of combined materials (see Fig. 4.62) gave 15% lower force peak than experiment.

However, there was a lot of simplifications starting with material models and ending with absence of the comfort padding and the retention system in the FE models of ČSN EN tests. These absences could have influence on obtained forces and deccelerations. Calculations suggest that proposed design is basically on the right way and insted of time consuming optimization of the material models, a prototype should be produced at this moment and real impact test should be performed to compare the model results and reality. Then it can be responsibly decided about the further change of the shape or materials.

5.4 Visualisation

Virtual CAD model was used to create the photorealistic renders. The construction and the main design features are summarized on Fig. 5.24. All possible configurations of the helmet are shown on Fig. 5.25 and Fig. 5.26 shows the adjustability of the peak and the visor.

Figure 5.24: Visualisation of the final design in the full configuration.

Figure 5.25: Visualisation of the final design in all configurations.

Figure 5.26: Visualisation of the final design in the full configuration. Ajustability of the visor.

The section through all assembly revealing all the layers can be seen on Fig. 5.27 and Fig. 5.28 shows the potentiall configuration of the helmet for the mountain rescue service in case the helmet passes ČSN EN 12 492 tests. Fig. 5.29 visualizes the final helmet design in detail with adjusted peak and no visor.

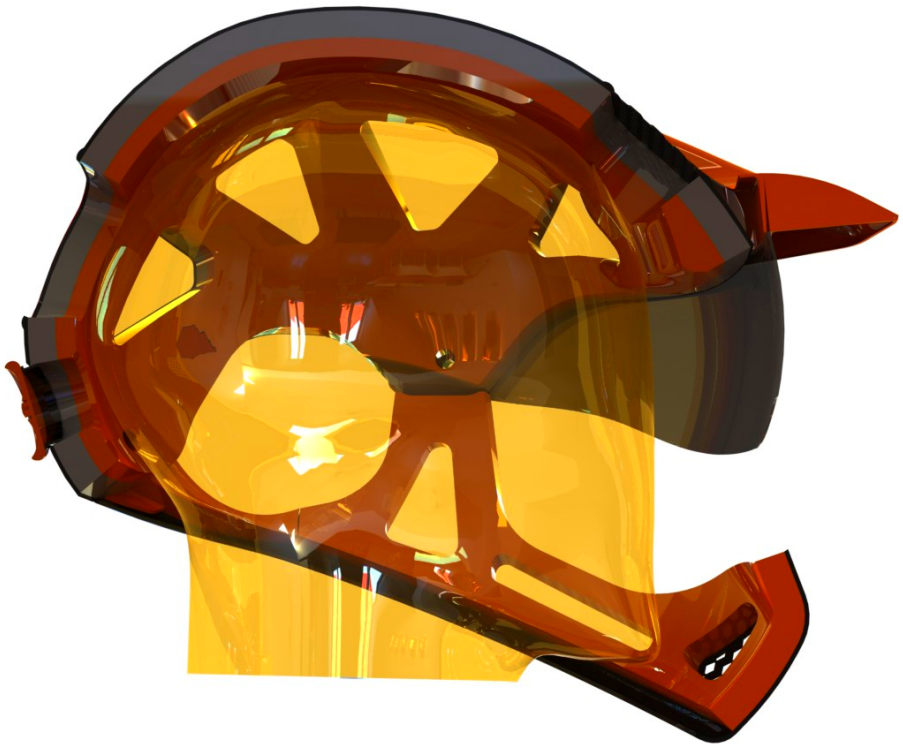

Figure 5.27: Visualisation of the section through the final design in the full configuration.

Figure 5.28: Visualisation of the configuration for mountain rescue service.

Figure 5.29: Visualisation of the final design.

Chapter 6

Conclusion

Seven sports (cycling, inline skating and skateboarding, mountaineering, horse riding, skiing and snowboarding, paragliding and white water sports) with combinable safety requirements were chosen as the target activities for which the versatile helmet was designed. Based on the research of the current state of the market and current technical solutions it was decided to use the combination of standart materials such as expanded polystyrene (EPS) and new materials like D3O.

EPS ensures ability to absorb the impact energy by the plastic deformation whereas D3O is able to absorb low energy impacts via it's viscoelasticity without any further consequences. Moreover, D3O plays a role of an insurance element in the case of multiple impact and penetration. Material parameters of EPS and D3O were identified using the results of the compression and impact tests and the optimization algorithm.

Safety and user requirements were included in the sketches of the versatile helmet and the best ones were later turned into the threedimensional CAD model. Using geometry of the model, finite element (FE) models of all standartized ČSN EN impact tests were created. The results of FE analysis showed that suggested design (total thickness of the helmet 19 mm, weight of the calculated configuration 375 g without peak, straps and retention system) would not pass the standards for the mountaineering helmets. Nevertheless, it is also explained that there are many simplifications that could influence the results.

Author of this thesis takes the view that further optimized and more detailed FE models would not be effective solution at the moment and the next steps should lead through the prototyping and real impact tests.

Bibliography

[1] Bicycle Helmet Safety Institute, information and images availabe at <http://www.helmets.org/>

[2] Information and images available at <http://www.paraevoluce.com>

[3] Information and images available at <http://www.protos.at>

[4] Information and images available at <http://www.nwsportx.com>

[5] Information and images available at <http://www.dainese.com>

[6] MICKA, M., JÍRA, J., JÍROVÁ, J., *Modelování pádové zkoušky helmy v Ansys LS Dyna*, ANSYS conference 2010, Frymburk 6. - 8. October 2010.

[7] Information and images available at <http://www.bikemag.com>

[8] Information and images available at <http://www.endurotribe.com>

[9] Information and images available at <http://www.hovding.com>

[10] Images available at <http://csmres.co.uk/cs.public.upd/article-images/Tenax-TPUD.jpg>

[11] Czech and European safety helmet standards *ČSN EN*

[12] LAŠ, V., *Mechanika kompozitních materiálů*, University of West Bohemia, 2008

[13] KOTTNER, R.: *Joining of Composite and Steel Machine Parts with Special Focus on Stiffness and Strength (in Czech)*, doctoral thesis, University of West Bohemia, Pilsen, 2007

[14] HYNEK, R.: *Strength design of composite rod*, bachelor thesis, University of West Bohemia, 2011

[15] RAMADAN, M., FA, Z., BAOZHONG, S., BOHONG, G.: *Finite element analyses of low-velocity impact damage of foam sandwiched composites with different ply angles face sheets*, Materials and Design 47 189–199, Elsevier, 2012

[16] HASHIN, Z., *Failure Criteria for Unidirectional Fiber Composites*, Journal of Applied Mwechanics 47(2), 329-334, 1980

[17] PINHO, S. T., ROBINSON, P., IANNUCCI, L., *Fracture toughness of the tensile and compressive fibre failure modes in laminated composites*, Department of Aeronautics, Imperial College London, UK

[18] DOLEO, F., FERABOLI, P., *Crashworthiness energy absorption of carbon fiber composites: experiment and simulation*, University of Washington, Seattle, WA 98195-2400

[19] JACOB, G. C., FELLERS, J. F., SIMUNOVIC, S., STARBUCK, J. M., *Energy Absorption in Polymer Materials for Automotive Crashworthiness*

[20] MAURIN, R., DAVIES, P., BARAL, N., BALEY, CH., *Transverse Properties of Carbon Fibres by Nano-Indentation and Micro-mechanics*, , Applied Composite Materials, Springer, 2008

[21] LANIER, B. K., *Study in the Improvement in Strength and Stiffness Capacity of Steel Multi-sided Monopole Towers Utilizing Carbon Fiber Reinforced Polymers as a Retrofitting Mechanism*

[22] ROSENBERG, J., LIŠKA, V. a kolektiv, *Experimentální chirurgie - nové technologie v medicíně. II. díl: Biomechanika*, Lékařská fakulta Univerzity Karlovy v Plzni, 2013

[23] *Simulia Abaqus/CAE 6.11 Documentation*

[24] NAGHIPOUR, P., SCHNEIDER, J., BARTSCH, M., HAUSMANN, J., VOGGENREITER, H., *Fracture simulation of CFRP laminates in mixed mode bending*, Engineering Fracture Mechanics, 2009

[25] Information and images available at < http://weburbanist.com/2009/06/16/10-fantastic-futuristic-materials-that-actually-exist/ >

[26] Information and images available at < http://www.d3o.com >

[27] MCINTOSH, A.S., ANDERSEN, T.E., BAHR R., et al., *Sport helmets now and in the future* Br J Sports Med, 45: 1258–1265

[28] Information and images available at < http://epsfoamprodotcom.sharepoint.com/Pages/ExpandedPolystyreneRawMaterialsResin.aspx >